# Epstein-Barr Virus Nuclear Antigen 1 (EBNA1) interacts with Regulator of Chromosome Condensation (RCC1) dynamically throughout the cell cycle

**Running title:** EBNA1 localizes with RCC1 to chromatin during mitosis

Thibaut Deschamps[1,3,4,5,6], Quentin Bazot[1,3,4,5,6¶], Derek M. Leske[7♦], Ruth MacLeod[7], Dimitri Mompelat[1,3,4,5,6♯], Lionel Tafforeau[2,3,6°], Vincent Lotteau[2,3,4,5,6], Vincent Maréchal[8], George S. Baillie[7], Henri Gruffat[1,3,4,5,6], Joanna B. Wilson[7] and Evelyne Manet[1,3,4,5,6*]

[1] CIRI, International Center for Infectiology Research, Oncogenic Herpesviruses team, Université de Lyon, Lyon, 69364, France

[2] CIRI, International Center for Infectiology Research, Cell Biology of Viral Infections team, Université de Lyon, Lyon, 69364, France

[3] INSERM, U1111, Lyon, 69364, France

[4] CNRS, UMR5308, Lyon, 69364, France

[5] Ecole Normale Supérieure de Lyon, Lyon, 69364, France

[6] Université Lyon 1, Centre International de Recherche en Infectiologie, Lyon, 69364, France

[7] College of Medical, Veterinary and Life Sciences, University of Glasgow, Glasgow G12 8QQ, UK

[8] UPMC Univ Paris 6, Inserm, Centre d'Immunologie et des Maladies Infectieuses (Cimi-Paris), UMR 1135, ERL CNRS 8255, F-75013 Paris, France

° Present address : Lionel Tafforeau, Cell Biology lab, University of Mons, Mons, Belgium

¶ Present address: Quentin Bazot, Section of Virology, Department of Medicine, Imperial College London, St Mary's Campus, London, UK

♯ Present address: University Joseph Fourier, Pathogenesis and Lentiviral Vaccination laboratory, Grenoble, France.

◆ University of Oxford, Ludwig Institute for Cancer Research, Oxford, United Kingdom

* corresponding author: Email: evelyne.manet@ens-lyon.fr ; Tel: +33 (0) 472 72 89 54

Keywords: Epstein-Barr virus, EBV, EBNA1, Regulator of Chromosome Condensation, RCC1

Subject category: animal/DNA viruses

Word count: 6496

## ABSTRACT

**The Epstein-Barr virus (EBV) nuclear antigen 1 (EBNA1) is a sequence-specific DNA binding protein which plays an essential role in viral episome replication and segregation, by recruiting the cellular complex of DNA replication onto the origin (*oriP)* and by tethering the viral DNA onto the mitotic chromosomes. Whereas the mechanisms of viral DNA replication are well documented, those involved in tethering EBNA1 to the cellular chromatin are far from being understood. Here, we have identified Regulator of Chromosome Condensation 1 (RCC1) as a novel cellular partner for EBNA1. RCC1 is the major nuclear guanine nucleotide exchange factor (RanGEF) for the small GTPase Ran enzyme. RCC1, associated with chromatin, is involved in the formation of RanGTP gradients critical for nucleo-cytoplasmic transport, mitotic spindle formation, and nuclear envelope reassembly following mitosis. Using several approaches, we have demonstrated a direct interaction between these two proteins and found that the EBNA1 domains responsible for EBNA1 tethering to the mitotic chromosomes are also involved in the interaction with RCC1. The use of an EBNA1 peptide array confirmed the interaction of RCC1 with these regions and also the importance of the N-terminal region of RCC1 in this interaction. Finally, using confocal microscopy and FRET analysis to follow the dynamics of interaction between the two proteins throughout the cell cycle, we have demonstrated that EBNA1 and RCC1 closely associate on the chromosomes during metaphase, suggesting an essential role for the interaction during this phase, perhaps in tethering EBNA1 to mitotic chromosomes.**


## INTRODUCTION

Epstein-Barr virus (EBV) is a ubiquitous herpesvirus associated with several human cancers (Crawford, 2001). Following primary infection, the virus persists in a life-long, latent state in

memory B cells, with intermittent viral production occurring in the oropharynx. *Ex vivo,* EBV has the capacity to induce growth transformation of resting primary human B-lymphocytes, leading to the establishment of lymphoblastoid cell lines (LCLs). In such cell lines, only a small number of viral genes are expressed which act in concert to induce and maintain continuous cell proliferation and survival (Kieff & Rickinson, 2007).

In latently infected cells, the EBV genome persists as a multicopy, covalently closed, double-stranded, nuclear episome. When cells proliferate, these episomes replicate once per cell-cycle during S phase, using the cellular DNA-replication machinery and are subsequently equally segregated to the daughter cells, such that a constant copy number of EBV genomes is maintained through cell divisions (Adams, 1987; Nanbo *et al.*, 2007; Yates & Guan, 1991). Both replication and segregation depend on the presence of two viral elements, the EBV *cis*-acting origin of plasmid replication (*oriP*) and the viral protein EBNA1 (Yates *et al.*, 1984, 1985). *oriP* is composed of two functional elements: the dyad symmetry (DS) element and the family of repeats (FR) (Reisman *et al.*, 1985). Both contain recognition sites for the EBNA1 protein. The DS element, which comprises four EBNA1 binding sites arranged in pairs, is required for DNA replication initiation (Rawlins *et al.*, 1985; Reisman *et al.*, 1985; Wysokenski & Yates, 1989; Chaudhuri *et al.*, 2001; Ritzi *et al.*, 2003; Schepers *et al.*, 2001). The FR element consists of an array of twenty imperfect 30 bp repeats, each one containing an 18 bp EBNA1 binding site (Rawlins *et al.*, 1985; Reisman *et al.*, 1985). FR functions by tethering the viral episomes to human metaphase chromosomes via EBNA1 (Sears *et al.*, 2003, 2004; Wu *et al.*, 2000, 2002) and this ensures the stable retention of *oriP*-episomes within the cells (Kirchmaier & Sugden, 1995; Little & Schildkraut, 1995; Nanbo *et al.*, 2007). FR is also required for EBNA1-dependent tethering of EBV genomes to specific perichromatic regions of host chromosomes during interphase (Deutsch et al, 2010) which appears to be essential for efficient replication of the episome (Hodin *et al.*, 2013).

EBNA1 is a homo-dimeric DNA-binding protein that recognises an 18 bp palindromic sequence *via* its C-terminal domain (residues 459-607 have been co-crystallised with DNA) (Ambinder *et al.*, 1990, 1991; Bochkarev *et al.*, 1996; Frappier & O'Donnell, 1991; Jones *et al.*, 1989; Rawlins *et al.*, 1985; Shah *et al.*, 1992). ChIPseq analyses have shown that, in addition to binding the DS and FR regions of *oriP*, EBNA1 binds multiple sites in the host genome (Lu *et al.*, 2010; Tempera *et al.*, 2015). Independently of its C-terminal-specific DNA-binding domain, EBNA1 can associate with chromatin throughout the cell cycle via its N-terminal half. This N-terminal region carries two domains, called Linking Regions 1 (LR1: aa 40-89) and 2 (LR2: aa 325-379) which confer intramolecular "linking" between EBNA1-DNA complexes as revealed by electrophoretic mobility shift assays (Mackey *et al.*, 1995). Each of these domains consists of a region rich in arginine and glycine (RGG-rich region: GR1 and GR2 respectively) and a unique region (UR1 and UR2 respectively). The RGG-rich regions possess intrinsic AT-hook activity allowing binding to AT-rich DNA (Sears *et al.*, 2003, 2004). These regions have been found to be important for EBNA1 replication and transcription activity (Mackey & Sugden, 1999) and to play an essential role in tethering EBNA1 to cellular DNA during interphase (Coppotelli *et al.*, 2011; Coppotelli *et al.*, 2013). EBNA1 attachment to metaphase chromosomes has been mapped to three independent chromosome binding sites (CBS) - CBS-1 (aa 72 to 84), CBS-2 (aa 328 to 365) and CBS-3 (aa 8 to 54) - that correlate well with the ability of EBNA1 to confer plasmid maintenance (Kanda *et al.*, 2001; Maréchal *et al.*, 1999; Wu *et al.*, 2002). However, the mechanisms responsible for EBNA1 interaction with mitotic chromosomes are still unclear. It has been proposed that the AT-hook structures within the LR1/LR2 regions could be directly responsible for EBNA1 attachment to the chromosomes (Kanda *et al.*, 2013; Sears *et al.*, 2004). Interestingly, HMGA1a a cellular chromatin-binding protein which associates with chromatin through its AT-hook domains, or histone H1, can functionally replace the amino

terminus of EBNA1 both in *oriP* plasmid replication and partitioning of the viral episome (Hung *et al.*, 2001; Sears *et al.*, 2003; Thomae *et al*., 2008). EBNA1 may also interact with chromatin through protein-protein interactions with one or several cellular partners. hEBP2 (human Epstein-Barr Binding Protein 2) was the first of the sort identified. (Kapoor *et al.*, 2005; Nayyar *et al.*, 2009; Wu *et al.*, 2000). hEBP2 binds to the LR2 region of EBNA1 (Shire *et al.*, 1999), which also corresponds to the CBS-2 region. In a yeast model, hEBP2 was required (in the presence of EBNA1) for the maintenance of a plasmid carrying the EBV FR sequence (Kapoor *et al.*, 2001, 2003). However, a recent study demonstrated that hEBP2 and EBNA1 do not interact during mitosis in living mitotic cells, suggesting that the involvement of hEPB2 might not be direct (Jourdan *et al.*, 2012; Frappier, 2012), or that it might have another role. More recently, HMGB2 (high-mobility group box 2), a well known chromatin component, has been identified as a new partner for EBNA1 (Jourdan *et al.*, 2012). EBNA1 interacts with HMGB2 on chromatin during interphase and mitosis, and its depletion partially alters EBNA1 association with the chromosomes. However, HMGB2 depletion is not sufficient to alter EBV episome maintenance in Raji cells (Jourdan *et al.*, 2012). Taken together, these results suggest that several mechanisms cooperate to promote EBNA1 association with the chromosomes throughout mitosis and maintenance of the EBV genome within proliferating cells.

In order to identify novel proteins that could play a role in EBNA1 chromosomal binding, we performed a yeast two-hybrid screen. From this screen, we identified Regulator of Chromosome Condensation 1 (RCC1), a major nuclear guanine nucleotide exchange factor (RanGEF) for the small GTPase Ran enzyme. In its association with chromatin, RCC1 is involved in the formation of RanGTP gradients critical for nucleo-cytoplasmic transport (Riddick & Macara, 2005), mitotic spindle formation and nuclear envelope reassembly after mitosis (Askjaer *et al.*, 2002; Bamba *et al.*, 2002). RCC1 is a ubiquitous nuclear protein

structured as a seven bladed propeller with unstructured small N- and C-terminal tails (Renault *et al.*, 1998). RCC1 directly interacts with histones H2A/H2B (Nemergut *et al.*, 2001) and its structure (bound to Ran and the nucleosomes) has been solved: one face of the protein binds to Ran (Renault *et al.*, 2001) whereas binding to chromatin involves the N-terminal tail of the protein as well as loop region in the fourth blade of its β-propeller (England *et al.*, 2010; Makde *et al.*, 2011). RCC1 is modified in cells by removal of the initial N-terminal methionine and mono-, di- or tri-methylation of the new N-terminal residue (serine 2 in human). This modification is present throughout the cell cycle and is necessary for stable chromatin association and normal mitosis (Chen *et al.*, 2007). The association of RCC1 with chromatin in interphase nuclei and mitotic chromosomes is highly dynamic (Cushman *et al.*, 2004; Li *et al.*, 2003) and regulated by its interaction with Ran (Hao & Macara, 2008; Zhang *et al.*, 2002). It is also regulated in a cell cycle dependent manner by various mechanisms including interaction with Ran-GTP-binding protein 1 (RanBP1) (Zhang *et al.*, 2014) and phosphoinositide 3-kinase beta (PI3Kβ) (Redondo-Muñoz *et al.*, 2015). A role of phosphorylation of serine 2 at the N-terminus of RCC1 has also been suggested but remains controversial (Bierbaum & Bastiaens, 2013; Hutchins *et al.*, 2004; Li & Zheng, 2004).

Due to its ability to interact with chromatin, especially through mitosis during which the interaction is stabilized, RCC1 appears to be a good candidate to promote the association of EBNA1 with chromatin. We have now confirmed the interaction between EBNA1 and RCC1 using various *in vitro* and *ex vivo* assays. We have demonstrated that this interaction is direct and characterized the domains involved. Finally, we found that although the proteins colocalized throughout the cell cycle, they only closely interact during metaphase, strongly suggesting a role for RCC1 in stabilizing the interaction between EBNA1 and the chromatin at this phase of the cell cycle.

## RESULTS

### Deletion of EBNA1 AT-hook motifs only partially modify its localization to the metaphasic chromosomes.

EBNA1 has been suggested to directly bind to AT-rich regions of the chromosomal DNA via AT-hook motifs located within the LR1/GR1 and LR2/GR2 regions (Sears *et al.*, 2004). In particular, fusion proteins between mCherry and various combinations of the EBNA1 regions containing AT-hook motifs, efficiently associated with chromosomes (Kanda *et al.*, 2013). However, the effect of specific deletion of these AT-hook motifs - in the context of the whole protein - on its association with cellular chromosomes has never been tested. We therefore generated derivatives of GFP-EBNA1 with either aa 40 to 53 (deleting most of GR1) or 326 to 358 (deleting two thirds of GR2) or both regions deleted (Fig. 1A) and tested their capacity to bind mitotic chromosomes and activate transcription. Association with chromosomes was first analysed by confocal microscopy, following transfection of HeLa cells with expression plasmids for GFP-EBNA1 or the mutated derivatives. Deletion of the GR regions led to the appearance of a faint diffuse staining of the cell nuclei which was more accentuated in the double mutant (Fig. 1B). However, even in the double mutant, a large proportion of the protein remained localized to the metaphasic chromosomes. This suggests that the AT-hook motifs are not the sole domains responsible for EBNA1 attachment to the chromosomes during mitosis. Second, we performed a FRAP analysis during cell interphase to comparatively evaluate the mobility of each protein. The half-time of fluorescence recovery of the EBNA1 GR-deletion mutants, especially that of the double mutant, was strongly diminished as compared with GR-wild type EBNA1, indicating a higher mobility of proteins lacking the AT-hook motifs (Fig. 1C). Finally, to complete the characterization of these mutants, we tested their transactivation ability since LR1 and LR2 regions were previously

reported to be important for transcriptional activation (Mackey & Sugden, 1999). The single GR deletion mutants appear to activate LUC expression from the pGL2-FR-TK-LUC reporter construct to similar levels as GR-wild type (Fig. 1D). By contrast the double mutant shows significant reduction in transcriptional activation through FR. Taken together, these results support a role for these two regions in transcriptional activation, but demonstrate that although these regions appear to play an important role in chromatin association during interphase, as could be deduced from the FRAP experiments, they are not absolutely essential for tethering EBNA1 to the mitotic chromosomes.

**EBNA1 interacts directly with RCC1**

Since the AT-hook motifs, appear not to be essential for EBNA1 association with mitotic chromatin, it is likely that one or more cellular partners are involved in mediating the linking of EBNA1 with the chromosomes. The two cellular proteins which have been previously found to play a role in this process - hEBP2 and HMGB2 - do not appear to be sufficient to account for all the properties of EBNA1 during EBV replication and segregation. In order to identify novel cellular partners of EBNA1, a yeast two-hybrid screen using EBNA1 as bait was performed. From this screen, Regulator of Chromosome Condensation 1 (RCC1) (gene ID: 1104), a guanine-nucleotide releasing factor that promotes exchange of Ran-bound GDP with GTP, was identified. RCC1 plays a key role both in nucleo-cytoplasmic transport and in the regulation of onset of chromosome condensation in S phase (Hadjebi *et al.*, 2008).

The interaction between EBNA1 and RCC1 was first examined by co-immunoprecipitation from transfected HeLa cells (Fig. 2A). Myc-tagged RCC1 specifically co-immunoprecipitated with Flag-tagged EBNA1. Consistently, in a reverse experiment, Myc-tagged EBNA1 specifically co-immunoprecipitated with Flag-tagged RCC1.

To assess if the interaction is direct, an *in vitro* GST-pulldown assay was performed using both GST-RCC1 and 6xhis-EBNA1 produced in bacteria and purified. 6xhis-EBNA1

was incubated with similar amounts of GST or GST-RCC1 proteins bound to glutathione sepharose beads. EBNA1 was efficiently retained on GST-RCC1 beads but not on GST alone, which strongly suggests that a direct interaction occurs between EBNA1 and RCC1 (Fig. 2B).

**EBNA1 binds RCC1 via domains previously reported to be essential for chromosome binding of the protein**

EBNA1 interaction with mitotic chromosomes has been reported to be dependent on three regions: CBS-1 (aa 72 to 84), CBS-2 (aa 328 to 365) and CBS-3 (aa 8 to 54) (Fig. 3A) (Kanda *et al.*, 2001; Maréchal *et al.*, 1999; Wu *et al.*, 2002). We thus investigated the involvement of these regions in the interaction with RCC1. For this, a series of GFP-tagged EBNA1 deletion mutants were expressed in HeLa cells and the lysates incubated with GST-RCC1-bound beads. Deletion mutants containing either CBS-1/CBS-3 (EBNA1 8-92), CBS-2 (EBNA1 323-410) or both (EBNA1 8-410) were all able to interact with RCC1, whereas EBNA1 377-641 with both regions deleted, showed considerably reduced interaction (Fig. 3B). This preferential interaction of RCC1 with the CBS domains of EBNA1 supports a putative role for RCC1 in EBNA1's targeting to metaphase chromosomes. Surprisingly however, deletion of region 326 to 376 completely abrogated the interaction with RCC1 (Fig. 3C), even though the CBS-1/-3 domains still present in this mutant were sufficient for interaction with RCC1 in mutant EBNA1 8-92 (Fig. 3B). This suggests that EBNA1 Δ326-376 protein's general topology may be altered such that the CBS-1/-3 domains are no longer accessible to interact with RCC1.

We also tested the capacity of the GR-deleted mutants used in Figure 1, to interact with RCC1 (Fig. 4). Although deletion of each region individually did not prohibit interaction with RCC1, deletion of both motifs had a dramatic effect. This suggests that at least one intact GR sub-region is required for the interaction with RCC1.

Taken together, these results indicate that the EBNA1 interaction domains with RCC1

overlap closely with the previously characterized EBNA1 chromosome binding regions. However, it is to be noted that mutant Δ40-53/Δ326-358 with GR1 and most of GR2 deleted, was still - at least partially - associated with the mitotic chromosome, whereas no interaction with RCC1 could be detected in the GST-pulldown assay. Thus, although RCC1 is likely to contribute to EBNA1 association with metaphasic chromosomes, it is probably not the only factor involved.

**The RCC1 N-terminal tail is essential for RCC1 interaction with EBNA1**

RCC1 is composed of small N-terminal and C-terminal unstructured tails surrounding a seven-bladed propeller structure (Makde *et al.*, 2011) (Fig. 5A). Due to the highly structured central domain of the protein, introducing large mutations into this region would likely disorder the entire structure. Therefore, a single RCC1 mutant, RCC1 Δ1-20, with the N-terminal tail deleted, was generated. Further, the N-terminal tail was cloned in fusion with GST. GST-pulldown using transfected HeLa cell extracts were performed with these proteins (Fig. 5B). Interestingly, we found that EBNA1 interacted strongly with the N-terminal tail of RCC1 and very inefficiently with the rest of the protein. To further map the interaction region, smaller deletions within the N-terminal extremity of RCC1 were introduced. Deletion of aa 11-15 or 16-20 did not significantly modify the interaction with EBNA1, in contrast to deletions of aa 1-5 and 6-10 which both impaired the interaction. These results suggest that the 10 first amino acids of the RCC1 N-terminal tail are important for the interaction of RCC1 with EBNA1.

**Peptide array analysis confirms the RCC1 interaction with the CBS-3/-1 and CBS-2 domains and also defines potential supplementary RCC1 interaction regions in the C-terminal moiety of the protein.**

With the aim to delimit the domains of EBNA1 involved in the interaction with RCC1 more precisely, a peptide array analysis was undertaken. A library of overlapping peptides (25-

mers), each shifted by 5 amino acids across the entire sequence of EBNA1 (including the GAr) was immobilised onto membranes and probed with recombinant GST-RCC1 full length (FL) and mutants (Fig. 6). Probing the EBNA1 peptide array with FL GST-RCC1 revealed intermediate to strong binding to peptides covering regions that encompass both GR repeats of EBNA1 as well as CBS-1 (aa 72 to 84) and CBS-3 (aa 8 to 54), which is consistent with our GST-pulldown mapping. It is interesting to note that the strongest interacting regions overlap with the AT-hook domains whose deletion in mutant EBNA1Δ40-53/Δ326-358, completely abrogates binding in our GST-pull down assay (Fig. 4). Thus, there is good agreement between the GST-pull down assay and the peptide array analysis. Moreover, the peptide analysis revealed the presence of unexpected binding regions in the central and C-terminal moiety of EBNA1: a first region between aa G371-E435 lies between the known binding sites for CK2 and USP7 and is well conserved in EBV EBNA1 isolates (Hussain *et al.*, 2014); a second region incorporates the C-terminal tail of the protein, rich in negatively charged residues. Reprobing the array with GST, indicated that the binding observed for GST-RCC1 was specific to RCC1.

When a second array was probed with GST-RCC1Δ1-20, binding was observed for largely the same set of peptides as for full length RCC1, but much weaker, with the notable exception of the C-terminal tail peptides, which showed no binding. Therefore, consistent with our GST-pulldown mapping, RCC1 with its N-terminal 20 aa deleted, only weakly interacts with EBNA1. This suggests that either the N-terminal region of RCC1 is the primary mediator of binding or that it is required for correct folding of full-length RCC1 to enable binding to EBNA1, or possibly both.

To distinguish between these possibilities, the second array was stripped and re-probed with just the N-terminal region of RCC1 fused to GST. GST-RCC1 1-20 showed intermediary binding to the C-terminal tail peptides and strong binding to peptides covering region R396 to

E435. However, strong binding was not observed with peptides localised in the N-terminal half of EBNA1 although these were strongly bound by full-length RCC1. This suggests that residues 1-20 of RCC1 contribute to the conformation of RCC1, or otherwise promote the full interaction, but may not completely comprise the binding site.

Regarding the strongest binding region identified for RCC1 1-20, analysis of the EBNA1 amino acid sequence reveals that the stretch of residues in common between EBNA1 peptides interacting strongly with GST-RCC1 1-20 lies between aa 411 to 420 (EADYFEYHQE). This region contains 4 negatively-charged residues. By contrast, the N-terminal region of RCC1 (MSPKRIAKRRSPPADAIPKS) contains 6 positively charged residues and one negatively charged residue. It is therefore possible that the interaction of RCC1 with these EBNA1 peptides is largely charge-based and possibly an artefact of the array approach, if these stretches are not normally accessible in the folded protein. To explore this possibility, a new array was generated with a series of mutated peptides spanning residue 401 to 430 and probed with GST-RCC1 1-20 (Supplementary Figure 1). This revealed that indeed charge is critical to the binding, such that replacement of the 4 charged residues ($E_{411}$, $D_{413}$, $E_{416}$, $E_{420}$) completely abrogated binding, however $F_{415}$ and $Y_{414}$ were also found to be key for the interaction. This region was thus a candidate for being a core binding site between the N-terminal region of RCC1 and EBNA1. However, an EBNA1 mutant deleted for this region (EBNA1Δ411-420) still interacted with RCC1 in a GST-pulldown assay (Fig. 4B, lane 5). Therefore, it appears that this region is not required for stabilizing the EBNA1-RCC1 interaction *in vitro*. However, it cannot be ruled out that it might play a role in the interaction *in vivo*, in a context where RCC1 is associated with chromatin.

**EBNA1 interacts with RCC1 localized to chromatin during mitosis**

In order to determine the subcellular localization of the two proteins in living cells, several fluorescent-tagged forms of EBNA1 and RCC1 were expressed in HeLa cells and

observed by live cell imaging during interphase and mitosis. The EGFP-RCC1 and EBNA1-RFP proteins colocalize almost perfectly in living cells during interphase and throughout mitosis (Fig. 7): during interphase the proteins colocalize throughout the nucleoplasm, with the exception of the nucleolus from which RCC1 is completely excluded and where weak staining is observed for EBNA1. During prophase and metaphase, both EBNA1 and RCC1 appear to be associated with the mitotic chromosomes. Similar observations were made in cells coexpressing other pairs of EGFP- and RFP-tagged forms of the proteins (data not shown).

To confirm that EBNA1 interacts with RCC1 in living cells we performed a Förster resonance energy transfer (FRET) analysis. FRET is a nonradioactive energy transfer that can occur when a donor and a compatible acceptor fluorophore are located at less than 10 nm from each other. FRET efficiency relies on the relative position and distance of the donor and acceptor fluorophores, which can be affected by the position of the fluorophore in a fusion protein. Therefore, both the following pairs of fusion proteins: EGFP-RCC1/EBNA1-RFP and EGFP-EBNA1/RFP-RCC1 were tested. No significant FRET was observed with the EGFP-RCC1/EBNA1-RFP pair. However, the EGFP-EBNA1/RFP-RCC1 pair revealed clear FRET activity during both interphase and metaphase (Fig. 8). During interphase, it is interesting to note that although the proteins colocalize throughout the nucleoplasm (Fig. 7), they were only in close interaction at the periphery of the nucleus (Fig. 8). Only very weak interaction was observed during prophase. By contrast, strong interaction was observed between the two proteins on metaphasic chromosomes. Taken together, these results suggest that the interaction between RCC1 and EBNA1 is highly dynamic through the cell cycle. The strong FRET signal observed specifically on metaphasic chromosomes supports a role for RCC1 in stabilizing the EBNA1 interaction with the chromosomes during mitosis.

## DISCUSSION

The mechanisms by which EBNA1 tethers the EBV genome to mitotic chromosomes are far from understood. The AT-hook regions of the protein have been proposed to play a major role in EBNA1 chromosome binding activity and episomal maintenance (Sears *et al.*, 2003, 2004). The use of netropsin, a small molecule that binds to the minor groove of AT-rich DNA, leads to the loss of EBV genomes from cells, supporting the role of the AT-hooks in episomal maintenance (Chakravorty & Sugden, 2015). However, we have found that deletion of the EBNA1 AT-hook regions does not abrogate EBNA1's general targeting to metaphasic chromosomes. This result is consistent with a previous analysis revealing three independent CBS regions (Marechal *et al.*, 1999). In effect, specific deletion of the AT-hook domains leaves CBS-1 (aa 72 to 84) intact. Therefore these data reinforce the idea of alternative or complementary mechanisms of recruitment of EBNA1 to the metaphasic chromosomes, possibly *via* the interaction with cellular chromatin binding factors.

Here, we have identified RCC1 as a novel mediator of EBNA1 interaction with metaphase chromosomes. We have characterized the interaction between EBNA1 and RCC1 by various methods. Importantly, by performing an *in vitro* assay using both proteins purified from bacteria, we have demonstrated that the two proteins can interact directly. Up to now, however, we have not been able to perform a successful co-immunoprecipitation with endogenous proteins. One explanation, other than a possible interference of antibodies with the interaction and the low level of expression of EBNA1, is the small amount of cells from the total population undergoing mitosis - the phase of the cell cycle in which our FRET experiments demonstrate a close interaction between the proteins.

Characterization of the interaction domains revealed that the RCC1 interaction domains of EBNA1 closely overlap with the CBS regions of the protein, known to be important for tethering EBNA1 to the chromosomes (Maréchal *et al.*, 1999). Accordingly, we have found

that region 8-92 which includes both CBS-3 and CBS-1, and region 323-410 which includes CBS-2, can interact independently with RCC1. Surprisingly, however, deletion of CBS-2 in mutant Δ326-376 previously found to impair hEBP2 interaction as well as *oriP* plasmid maintenance and mitotic localization (Shire *et al.*, 1999; Wu *et al.*, 2000), completely abolished EBNA1 interaction with RCC1. This latter result is not consistent with the finding that the CBS-3/-1 region (still present in this mutant) is sufficient alone to mediate the interaction with RCC1. This suggests that the conformation or accessibility of the CBS-3/-1 region is compromised in this mutant, affecting various functions of the protein without necessarily reflecting the direct involvement of the deleted region.

Since the EBNA1 mutant with the two AT-hook domains deleted, appears to localize to chromatin both during interphase and through mitosis (which had not previously been tested), mechanisms other than the interaction of EBNA1 with AT-rich regions of DNA are likely to be required. However, deletion of the two AT-hook domains also affected the interaction with RCC1, suggesting that still other factors are involved. Another chromatin binding protein, HMGB2, was previously identified as an EBNA1 interacting factor (Jourdan *et al.*, 2012). HMGB2 could thus be responsible for targeting EBNA1 to the chromatin, in the absence of both direct interaction with DNA (via the AT-hooks) and interaction with RCC1. To corroborate such an hypothesis it would be interesting to know more precisely where HMGB2 binds within EBNA1. Alternatively, another as yet unidentified partner could be involved in the process. These possibilities are not mutually exclusive, indeed EBNA1 may employ multiple mechanisms to tether the viral genome to chromatin and to associate with the chromatin independently of the viral genome, through the different stages of the cell cycle and under various conditions.

Regarding the domains of RCC1 involved in the interaction with EBNA1, the N-terminal flexible region of RCC1 was identified as an essential domain. Interestingly, this N-

terminal tail, and in particular the serine at position 2, is the site of post-transcriptional modifications (both α-N-methylation and phosphorylation) that are important for stable chromatin association and regulation of RCC1's NLS interaction with importins α and β (Chen *et al.*, 2007; Li & Zheng, 2004). Such modifications of RCC1 N-terminal tail within mammalian cells could modulate or even prevent the interaction between the two proteins. Conversely, since these modifications have been suggested to play an important role in the mobility of RCC1 during metaphase and in its stabilization on the chromatin (Hutchins *et al.*, 2004; Li & Zheng, 2004), EBNA1's interaction with these regions could affect the dynamics of RCC1's interaction with chromatin.

Use of EBNA1 peptide arrays permitted a more detailed mapping of the EBNA1 interaction regions with respect to full length RCC1 as well as the N-terminal tail. Interaction of full-length RCC1 (and to lesser extent the N-terminal tail of RCC1 alone) with the CBS-1/-3 and CBS-2 regions of EBNA1 was confirmed. In addition, two other regions of EBNA1 were identified that might be involved in the interaction: the C-terminal tail, and a negatively charged region located between the previously characterized CK2 and USP7 binding sites. Interestingly, these two regions (particularly the latter) are recognised by RCC1's N-terminal tail. In particular, the N-terminal tail of RCC1 critical for the interaction specifically contacts a region of EBNA1 - DYFEYHQE - located between aa 413 and 420. When set in the context of an *in silico* structural model of full-length EBNA1 (Hussain *et al.*, 2014), this domain appears to be located in a region that resembles a small pocket. This could potentially accommodate the N-terminal region of RCC1, facilitating further interactions between the CBS domains of EBNA1 and the seven-propeller helix of RCC1, and hence stabilising the interaction between the two proteins. However, deletion of this domain does not preclude binding of EBNA1 and RCC1 in the *in vitro* assays used here and we cannot exclude that it may reflect artifactual binding to a site that is not normally accessible to RCC1.

With regard to the dynamics of interaction between the two proteins in live cells, the combination of colocalization experiments in live cells and FRET analysis reveals that the two proteins colocalize with the chromatin throughout the cell cycle. However, their proximity varies according to the location within the cell nucleus as well as the phase of the cell cycle: during interphase, although the two proteins appear to be colocalizing throughout the cell nucleus, FRET could only be observed at the periphery of the nucleus, suggesting that close interaction between EBNA1 and RCC1 could be linked to the latter being in a different conformation when actively involved in nucleo-cytoplasmic transport. This result opens up the possibility that the interaction of EBNA1 with RCC1 could play a role in functions other than segregation of the viral episome.

Importantly, during mitosis, FRET was mainly observed in metaphase, indicating a more specific role for the RCC1-EBNA1 interaction at this particular stage of mitosis that precedes segregation of sister chromatids. This observation, together with the correlation between EBNA1 regions interacting with RCC1 and EBNA1 domains previously characterized for their role in chromosome binding and episome maintenance, argues for an important role of RCC1 in EBV episome tethering to the chromosomes and subsequent episome maintenance. However, this hypothesis will be difficult to prove directly since RCC1 is an essential protein whose downregulation leads to premature chromosome condensation or arrest in the G1 phase of the cell cycle (Uchida *et al.*, 1990). The observation that deletion of the AT-hook domains still permits association of EBNA1 with metaphase chromosomes while it appears to abrogate interaction with RCC1 *in vitro*, does not refute the hypothesis. First, the assay conditions used to detect the interaction *in vitro* may not be optimum and a weak interaction between EBNA1 and RCC1 might nevertheless occur *in vivo* in the absence of the AT-hook domains. Alternatively, in the absence of an interaction between RCC1 and EBNA1, alternative mechanisms tethering EBNA1 to the chromatin may act. Of note, depletion of

HMGB2 was found to affect the stability but not to prevent EBNA1 association with chromatin, nor did it impact viral genome maintenance, despite the observed interaction between EBNA1 and HMGB2 on chromatin through mitosis (Jourdan *et al.*, 2012). It is thus likely that several mechanisms are involved in EBNA1 tethering to the chromatin, orchestrated to play a role at different stages of the cell cycle to both bring EBNA1 to the chromatin and stabilize it once there: During interphase, the EBV genomes are distributed to perichromatic regions of the nucleus in a manner dependent on the FR element and EBNA1 (Deutsch *et al*., 2010). It has been suggested that the AT-hook domains of EBNA1 could play an important role in this tethering of the EBV genomes to the chromatin. This hypothesis is strengthened by the demonstration that HMG1Aa, an AT-hook binding protein can functionally replace the N-terminal domain of EBNA1 (Sears *et al.*, 2003; Thomae *et al*., 2008) and by the results of our FRAP analysis showing a higher mobility of EBNA1 with its AT-hook domains deleted; HMGB2 is associated with EBNA1 on the chromatin during interphase and more so during mitosis (Jourdan *et al.*, 2012); RCC1 colocalizes with EBNA1 throughout the cell cycle but the interaction appears to be specifically stabilized during metaphase. Moreover, interaction between EBNA1 and the chromatin could be facilitated by a direct interaction through the AT-hook domains with nucleosomal DNA.

Finally, it is interesting to note that the ortholog of EBNA1 in KSHV (Kaposi Sarcoma Herpes Virus), LANA (Latency-Associated Nuclear antigen), directly interacts with H2A-H2B dimers to enable its binding to chromosomes (Piolot *et al.*, 2001). The resolution of the crystal structure of the nucleosome complexed with the first 23 amino acids of LANA revealed that the LANA peptide forms a hairpin that interacts with an acidic H2A-H2B region implicated in the formation of higher order chromatin structure (Barbera *et al.*, 2006). Interestingly, RCC1 targets the same region of the nucleosomal H2A-H2B dimer as LANA, and the two proteins have been shown to compete for nucleosome interaction (England *et al.*,

2010). Thus, whereas LANA directly contacts the H2A-H2B dimer to enable its binding to the chromosomes, EBNA1 may interact indirectly with the same H2A-H2B dimer through RCC1. Similar to EBNA1, LANA also interacts with several cellular proteins that appear to play a role in the tethering of LANA to chromosomes and/or episomal segregation (Krithivas *et al.*, 2002; Xiao *et al.*, 2010). Thus EBNA1 and LANA have evolved similar but not identical mechanisms to insure anchorage of the viral episomes onto the chromatin at different stages of the cell cycle, allowing efficient replication and segregation of the respective viral genomes.

## METHODS

### Cell culture and transfections

HeLa and HEK293T cells were grown at 37°C in DMEM, 10% FCS. Plasmid transfection was performed using the PEI transfection reagent (Polysciences).

### Plasmids

pEGFP-N1-EBNA1ΔGA (aa 8 to 641) has been described previously (Jourdan *et al.*, 2012). Unless otherwise indicated, all EBNA1 plasmids used were derived from this plasmid and thus contain EBNA1 deleted for GAr as well as the first 7 N-terminal aa. EBNA1 and RCC1 N-terminal tail deletion mutants were generated by site-directed mutagenesis (QuickChange Site-Directed Mutagenesis kit, Stratagene). For the two-hybrid screen, ORFs for EBNA1, EBNA1 8-410 and EBNA1-381Cter were PCR-amplified (KOD Hot Start DNA Polymerase®, EMD Millipore) cloned first in pDONR207 then into pGBKT7, using the Gateway recombinational cloning system (Invitrogen). EBNA1 and deletion mutants cloned into pDEST-Myc, pCI-3xFlag, pDEST15 or pDEST53 were also generated using the Gateway system. A codon-optimised version of EBNA1-ΔGA was cloned into pET22b (Merck Millipore) to generate pET22b-EBNA1. The ORF for full-length RCC1 (alpha isoform) was

transferred from pDONR223-RCC1 (obtained from a human ORFeome library) into pDEST-Myc, pCI-3xFlag or pDEST$^{TM}$15 (Invitrogen) using the Gateway system. pEGFP-C1-EBNA1 has been described previously (Jourdan *et al.*, 2012). pRFP and pEGFP fusion proteins were generated by cloning the relevant PCR-amplified ORFs in pRFP-N1, pRFP-C1, pEGFP-N1 or pEGFP-C1, using the In-Fusion®HD cloning kit (Clontech). All oligonucleotides used are listed in Supplementary Table 1.

**Luciferase Assays**

Renilla or Firefly luciferase activities were measured in a Veritas$^{TM}$ Luminometer (Turner Biosystems) using the Renilla or Firefly Luciferase Assay system (Promega Madison Co).

**Yeast two-hybrid screens**

The screens were performed as previously described (Bazot *et al.*, 2014) using pGBKT7-EBNA1/-EBNA1-8-410 or -EBNA1-381Cter as bait vectors and a human LCL AD-cDNA library (Invitrogen). Positive clones were sequenced and identified by automatic BLAST (Pellet *et al.*, 2010).

**Co-immunoprecipitation and western blotting**

Cells were lysed in 50 mM Tris-HCl pH 7.5, 150-300 mM NaCl, 1 mM Dithiotreitol (DTT) and 0.5% Nonidet P-40 plus protease inhibitors. For immunoprecipitation of transiently expressed Flag-tagged proteins, extracts were incubated with 20 µl of anti-Flag M2 affinity gel (Sigma) for 4 h at 4°C. After washing, bound proteins were analysed by western blotting, visualised using ECL (Thermo Fisher Scientific). Antibodies: anti-Flag rabbit polyclonal antibody (Sigma), anti-His6 mouse monoclonal antibody (Roche Molecular Biochemicals), anti-c-Myc (9E10) HRP-conjugated antibody (Santa Cruz Biotechnology, Inc). Anti-rabbit and anti-mouse (HRP)-conjugated antibodies (GE Healthcare) were used as secondary antibodies.

**Production and purification of the 6xhis-EBNA1 protein**

6xhis-EBNA1 was purified from *Escherichia coli* Rosetta (pLysS) strain transformed with pET22b-EBNA1. Cells were lysed in 50 mM NaH2PO4, 1 M NaCl, 10 mM imidazole pH 8, protease inhibitors and 1 mg/ml lysozyme. After sonication, the protein was purified by gravity-flow chromatography using Ni-NTA agarose beads. Beads were washed with lysis buffer plus 50 mM imidazole and the proteins eluted in lysis buffer containing 150 mM imidazole.

***In vitro* GST-Pulldowns**

Glutathione S-Transferase (GST) and GST-fusion proteins were purified from *Escherichia coli* BL21 (DE3) codon plus strain extracts, with glutathione-Sepharose 4B beads (GE Healthcare). Beads carrying the GST or the GST-fusion proteins were equilibrated in MTPBS (150 mM NaCl, 16 mM $Na_2HPO_4$, 4 mM $NaH_2PO_4$, 100 mM EDTA, 1% Triton) and incubated with either purified 6xhis-EBNA1 or transfected cell extracts for 4h in MTPBS. Beads were washed 5 times in MTPBS and bound proteins analysed by western blotting.

**EBNA1 peptides arrays**

25mer peptides comprising the entire sequence of EBNA1 (B95.8 strain), with 5 residue shifts (ie. initiating at residues 1, 6, 11, 16 etc) were synthesized by automatic SPOT synthesis (Kramer and Schneider-Mergener, 1998) directly onto cellulose membranes using Fmoc (9-fluorel methoxycarbonyl) chemistry and Autospot Robot ASS222 peptide synthetizer (Invatis Bioanalytical Instruments AG). Arrays were bathed in ethanol and washed for 10 mins in TBST (50 mM Tris.HCl pH7.5, 150 mM NaCl, 0,05% Tween-20), followed by blocking in TBST, 5% non-fat milk powder (NFM) for 2 hours at RT and washed again with TBST. Arrays were probed with purified GST (as control) or GST fusion proteins, at 2 to 5 ug/mL in TBST, 1% NFM, shaking overnight at 4°C. After washing in TBST, membranes were incubated with rabbit anti-GST-HRP and the array revealed using ECL (Pierce #32106). To strip the array membranes for re-probing, they were covered in 60 mM Tris-HCl pH6.8, 20

539 mM DTT, 70 mM SDS, at 70°C for 30 min.

540 **Confocal microscopy**

541 HeLa cells were plated onto glass-bottomed dishes for confocal microscopy (Ibidi) and
542 transfected with expression vectors coding for EBNA1 and RCC1 fused to either EGFP or
543 RFP. Live cells were analyzed with a Zeiss LSM710 confocal microscope with ZEN software.
544 GFP and RFP signals were acquired using respectively an argon laser at 488nm and a laser
545 diode (DPSS) at 561nm. Z-stack series were also acquired for mitotic cells: the most
546 representative stacks are presented. All analyses were conducted with ImageJ Software.

547 **Fluorescence recovery after photobleaching (FRAP) analysis**

548 Cells used for FRAP acquisition were prepared as for classical microscopy and data collected
549 using a confocal spinning disk microscope. Same parameters were used to acquire all images.
550 Regions of interest were photobleached using a 494-nm laser during 510ms at full power.
551 Images were acquired with an EM gain of 30, 200ms exposure time and a 488-nm laser at
552 9.5% full power. 5 images were acquired before bleaching then 1 image every 0.5s for 5
553 seconds, 1 image per second for 1 minute and 1 image every 5 seconds for 30 seconds.
554 Analysis was performed using ImageJ and EasyFrap software.

555 **Förster resonance energy transfer (FRET) analysis**

556 Cells used for FRET acquisition were prepared as for confocal microscopy and data collected
557 with an LSM-710 confocal microscope. FRET analysis was performed using the FRET
558 Analyzer plugin (http://rsb.info.nih.gov/ij/plugins/fret-analyzer/fret-analyzer.htm). Three
559 tracks were used for the acquisition: EGFP (excitation: GFP, reception: GFP range), RFP
560 (excitation: RFP, reception: RFP range) and FRET (excitation: GFP, reception: RFP range).
561 Argon laser and DPSS were used at 2% and 7% power respectively. Gain level was 540 for
562 the GFP signal and 640 or 690 for the RFP signal. Spectral leakage was measured by
563 acquisition of 5 images for each track with EGFP or RFP fusions expressed alone. Double

transfected cells were used for FRET acquisition data. In each case EGFP, RFP and FRET fluorescent signals were acquired for each track.

## ACKNOWLEDGEMENTS

This work was supported by the 'Institut National de la Santé et de la Recherche Médicale' (INSERM); 'the Cluster de Recherche Rhône-Alpes en Infectiologie'; 'the Ligue Contre le Cancer, comité du Rhône'; the 'Association pour la Recherche contre le Cancer (ARC grant n° R11176CC)'. T. D. and Q. B. have been recipient of a fellowship from the 'Ministère de l'enseignement et de la Recherche scientifique (MENRS), T. B. from the "Ligue Nationale Contre le Cancer", Q. B. from the 'Association pour la Recherche contre le Cancer' and D. M. L. by a Medical Research Council (MRC) scholarship. We acknowledge the AniRA Genetic Analysis and cytometry platforms and the "Platim" microscope facilities of the SFR Biosciences Gerland-Lyon Sud (US8/UMS3444).

## REFERENCES

**Adams, A. (1987).** Replication of latent Epstein-Barr virus genomes in Raji cells. *J Virol* **61**, 1743–1746.

**Ambinder, R. F., Shah, W. A., Rawlins, D. R., Hayward, G. S. & Hayward, S. D. (1990).** Definition of the sequence requirements for binding of the EBNA-1 protein to its palindromic target sites in Epstein-Barr virus DNA. *J Virol* **64**, 2369–2379.

**Ambinder, R. F., Mullen, M. A., Chang, Y. N., Hayward, G. S. & Hayward, S. D. (1991).** Functional domains of Epstein-Barr virus nuclear antigen EBNA-1. *J Virol* **65**, 1466–1478.

**Askjaer, P., Galy, V., Hannak, E. & Mattaj, I. W. (2002).** Ran GTPase cycle and importins alpha and beta are essential for spindle formation and nuclear envelope assembly in living Caenorhabditis elegans embryos. *Mol Biol Cell* **13**, 4355–4370.

**Bamba, C., Bobinnec, Y., Fukuda, M. & Nishida, E. (2002).** The GTPase Ran regulates chromosome positioning and nuclear envelope assembly in vivo. *Curr Biol CB* **12**, 503–507.

**Barbera, A. J., Chodaparambil, J. V., Kelley-Clarke, B., Joukov, V., Walter, J. C., Luger, K. & Kaye, K. M. (2006).** The nucleosomal surface as a docking station for Kaposi's sarcoma herpesvirus LANA. *Science* **311**, 856–861.

**Bazot, Q., Deschamps, T., Tafforeau, L., Siouda, M., Leblanc, P., Harth-Hertle, M. L., Rabourdin-Combe, C., Lotteau, V., Kempkes, B. & other authors**. **(2014).** Epstein-Barr virus nuclear antigen 3A protein regulates CDKN2B transcription via interaction with MIZ-1. *Nucleic Acids Res* **42**, 9700–9716.

**Bierbaum, M. & Bastiaens, P. I. H. (2013).** Cell cycle-dependent binding modes of the ran exchange factor RCC1 to chromatin. *Biophys J* **104**, 1642–1651.

**Bochkarev, A., Barwell, J. A., Pfuetzner, R. A., Bochkareva, E., Frappier, L. & Edwards, A. M. (1996).** Crystal structure of the DNA-binding domain of the Epstein-Barr virus origin-binding protein, EBNA1, bound to DNA. *Cell* **84**, 791–800.

**Cai, X., Schafer, A., Lu, S., Bilello, J. P., Desrosiers, R. C., Edwards, R., Raab-Traub, N. & Cullen, B. R. (2006).** Epstein-Barr virus microRNAs are evolutionarily conserved and differentially expressed. *PLoS Pathog* **2**, e23.

**Chakravorty, A. & Sugden, B. (2015).** The AT-hook DNA binding ability of the Epstein Barr virus EBNA1 protein is necessary for the maintenance of viral genomes in latently infected cells. *Virology* **484**, 251–258.

**Chaudhuri, B., Xu, H., Todorov, I., Dutta, A. & Yates, J. L. (2001).** Human DNA replication initiation factors, ORC and MCM, associate with oriP of Epstein-Barr virus. *Proc Natl Acad Sci U S A* **98**, 10085–10089.

**Chen, T., Muratore, T. L., Schaner-Tooley, C. E., Shabanowitz, J., Hunt, D. F. & Macara, I. G. (2007).** N-terminal alpha-methylation of RCC1 is necessary for stable

614 chromatin association and normal mitosis. *Nat Cell Biol* **9**, 596–603.

615 **Coppotelli, G., Mughal, N., Marescotti, D. & Masucci, M. G. (2011).** High avidity binding
616 to DNA protects ubiquitylated substrates from proteasomal degradation. *J Biol Chem* **286**,
617 19565–19575.

618 **Coppotelli, G., Mughal, N. & Masucci, M. G. (2013).** The Gly-Ala repeat modulates the
619 interaction of Epstein-Barr virus nuclear antigen-1 with cellular chromatin. *Biochem Biophys*
620 *Res Commun* **431**, 706–711.

621 **Crawford, D. H. (2001).** Biology and disease associations of Epstein-Barr virus. *Philos*
622 *Trans R Soc Lond B Biol Sci* **356**, 461–73.

623 **Cushman, I., Stenoien, D. & Moore, M. S. (2004).** The dynamic association of RCC1 with
624 chromatin is modulated by Ran-dependent nuclear transport. *Mol Biol Cell* **15**, 245–255.

625 **Deutsch, M. J., Ott, E. & Schepers, A. (2010).** The latent origin of replication of Epstein-
626 Barr virus directs viral genomes to active regions of the nucleus. *J Virol* **84**, 2533-2546.

627 **England, J. R., Huang, J., Jennings, M. J., Makde, R. D. & Tan, S. (2010).** RCC1 uses a
628 conformationally diverse loop region to interact with the nucleosome: a model for the RCC1-
629 nucleosome complex. *J Mol Biol* **398**, 518–29.

630 **Frappier, L. & O'Donnell, M. (1991).** Overproduction, purification, and characterization of
631 EBNA1, the origin binding protein of Epstein-Barr virus. *J Biol Chem* **266**, 7819–7826.

632 **Hadjebi, O., Casas-Terradellas, E., Garcia-Gonzalo, F. R. & Rosa, J. L. (2008).** The
633 RCC1 superfamily: from genes, to function, to disease. *Biochim Biophys Acta* **1783**, 1467–79.

634 **Hao, Y. & Macara, I. G. (2008).** Regulation of chromatin binding by a conformational
635 switch in the tail of the Ran exchange factor RCC1. *J Cell Biol* **182**, 827–36.

636 **Hodin, T. L., Najrana, T. & Yates, J. L. (2013).** Efficient replication of Epstein-Barr virus-
637 derived plasmids requires tethering by EBNA1 to host chromosomes. *J Virol* **87**, 13020–
638 13028.

**Hung, S. C., Kang, M. S. & Kieff, E. (2001).** Maintenance of Epstein-Barr virus (EBV) oriP-based episomes requires EBV-encoded nuclear antigen-1 chromosome-binding domains, which can be replaced by high-mobility group-I or histone H1. *Proc Natl Acad Sci U S A* **98**, 1865–1870.

**Hussain, M., Gatherer, D. & Wilson, J. B. (2014).** Modelling the structure of full-length Epstein-Barr virus nuclear antigen 1. *Virus Genes* **49**, 358–372.

**Hutchins, J. R. A., Moore, W. J., Hood, F. E., Wilson, J. S. J., Andrews, P. D., Swedlow, J. R. & Clarke, P. R. (2004).** Phosphorylation regulates the dynamic interaction of RCC1 with chromosomes during mitosis. *Curr Biol CB* **14**, 1099–1104.

**Jones, C. H., Hayward, S. D. & Rawlins, D. R. (1989).** Interaction of the lymphocyte-derived Epstein-Barr virus nuclear antigen EBNA-1 with its DNA-binding sites. *J Virol* **63**, 101–110.

**Jourdan, N., Jobart-Malfait, A., Dos Reis, G., Quignon, F., Piolot, T., Klein, C., Tramier, M., Coppey-Moisan, M. & Maréchal, V. (2012).** Live-cell imaging reveals multiple interactions between Epstein-Barr virus nuclear antigen 1 and cellular chromatin during interphase and mitosis. *J Virol* **86**, 5314–5329.

**Kanda, T., Otter, M. & Wahl, G. M. (2001).** Coupling of mitotic chromosome tethering and replication competence in epstein-barr virus-based plasmids. *Mol Cell Biol* **21**, 3576–3588.

**Kanda, T., Horikoshi, N., Murata, T., Kawashima, D., Sugimoto, A., Narita, Y., Kurumizaka, H. & Tsurumi, T. (2013).** Interaction between basic residues of Epstein-Barr virus EBNA1 protein and cellular chromatin mediates viral plasmid maintenance. *J Biol Chem* **288**, 24189–24199.

**Kapoor, P. & Frappier, L. (2003).** EBNA1 partitions Epstein-Barr virus plasmids in yeast cells by attaching to human EBNA1-binding protein 2 on mitotic chromosomes. *J Virol* **77**, 6946–56.

**Kapoor, P., Shire, K. & Frappier, L. (2001).** Reconstitution of Epstein-Barr virus-based plasmid partitioning in budding yeast. *EMBO J* **20**, 222–30.

**Kapoor, P., Lavoie, B. D. & Frappier, L. (2005).** EBP2 plays a key role in Epstein-Barr virus mitotic segregation and is regulated by aurora family kinases. *Mol Cell Biol* **25**, 4934–4945.

**Kieff, E. & Rickinson, A. B. (2007).** Epstein Barr virus and its replication. In *Fields Virol*, pp. 2063–2654. Edited by D. M. Knipe. Wolters Kluwer/ Lippincott Williams &Wilkins.

**Kirchmaier, A. L. & Sugden, B. (1995).** Plasmid maintenance of derivatives of oriP of Epstein-Barr virus. *J Virol* **69**, 1280–1283.

**Krithivas, A., Fujimuro, M., Weidner, M., Young, D. B. & Hayward, S. D. (2002).** Protein interactions targeting the latency-associated nuclear antigen of Kaposi's sarcoma-associated herpesvirus to cell chromosomes. *J Virol* **76**, 11596–11604.

**Li, H. Y. & Zheng, Y. (2004).** Phosphorylation of RCC1 in mitosis is essential for producing a high RanGTP concentration on chromosomes and for spindle assembly in mammalian cells. *Genes Dev* **18**, 512–27.

**Li, H. Y., Wirtz, D. & Zheng, Y. (2003).** A mechanism of coupling RCC1 mobility to RanGTP production on the chromatin in vivo. *J Cell Biol* **160**, 635–44.

**Little, R. D. & Schildkraut, C. L. (1995).** Initiation of latent DNA replication in the Epstein-Barr virus genome can occur at sites other than the genetically defined origin. *Mol Cell Biol* **15**, 2893–2903.

**Lu, F., Wikramasinghe, P., Norseen, J., Tsai, K., Wang, P., Showe, L., Davuluri, R. V. & Lieberman, P. M. (2010).** Genome-wide analysis of host-chromosome binding sites for Epstein-Barr Virus Nuclear Antigen 1 (EBNA1). *Virol J* **7**, 262.

**Mackey, D. & Sugden, B. (1999).** The linking regions of EBNA1 are essential for its support of replication and transcription. *Mol Cell Biol* **19**, 3349–3359.

**Mackey, D., Middleton, T. & Sugden, B. (1995).** Multiple regions within EBNA1 can link DNAs. *J Virol* **69**, 6199–6208.

**Makde, R. D., England, J. R., Yennawar, H. P. & Tan, S. (2011).** Structure of RCC1 chromatin factor bound to the nucleosome core particle. *Nature* **467**, 562–6.

**Maréchal, V., Dehee, A., Chikhi-Brachet, R., Piolot, T., Coppey-Moisan, M. & Nicolas, J. C. (1999).** Mapping EBNA-1 domains involved in binding to metaphase chromosomes. *J Virol* **73**, 4385–92.

**Nanbo, A., Sugden, A. & Sugden, B. (2007).** The coupling of synthesis and partitioning of EBV's plasmid replicon is revealed in live cells. *EMBO J* **26**, 4252–4262.

**Nayyar, V. K., Shire, K. & Frappier, L. (2009).** Mitotic chromosome interactions of Epstein-Barr nuclear antigen 1 (EBNA1) and human EBNA1-binding protein 2 (EBP2). *J Cell Sci* **122**, 4341–50.

**Nemergut, M. E., Mizzen, C. A., Stukenberg, T., Allis, C. D. & Macara, I. G. (2001).** Chromatin docking and exchange activity enhancement of RCC1 by histones H2A and H2B. *Science* **292**, 1540–1543.

**Pellet, J., Tafforeau, L., Lucas-Hourani, M., Navratil, V., Meyniel, L., Achaz, G., Guironnet-Paquet, A., Aublin-Gex, A., Caignard, G. & other authors. (2010).** ViralORFeome: an integrated database to generate a versatile collection of viral ORFs. *Nucleic Acids Res* **38**, D371–8.

**Piolot, T., Tramier, M., Coppey, M., Nicolas, J. C. & Marechal, V. (2001).** Close but distinct regions of human herpesvirus 8 latency-associated nuclear antigen 1 are responsible for nuclear targeting and binding to human mitotic chromosomes. *J Virol* **75**, 3948–3959.

**Rawlins, D. R., Milman, G., Hayward, S. D. & Hayward, G. S. (1985).** Sequence-specific DNA binding of the Epstein-Barr virus nuclear antigen (EBNA-1) to clustered sites in the plasmid maintenance region. *Cell* **42**, 859–868.

**Redondo-Muñoz, J., Pérez-García, V., Rodríguez, M. J., Valpuesta, J. M. & Carrera, A. C. (2015).** Phosphoinositide 3-kinase beta protects nuclear envelope integrity by controlling RCC1 localization and Ran activity. *Mol Cell Biol* **35**, 249–263.

**Reisman, D., Yates, J. & Sugden, B. (1985).** A putative origin of replication of plasmids derived from Epstein-Barr virus is composed of two cis-acting components. *Mol Cell Biol* **5**, 1822–1832.

**Renault, L., Nassar, N., Vetter, I., Becker, J., Klebe, C., Roth, M. & Wittinghofer, A. (1998).** The 1.7 A crystal structure of the regulator of chromosome condensation (RCC1) reveals a seven-bladed propeller. *Nature* **392**, 97–101.

**Renault, L., Kuhlmann, J., Henkel, A. & Wittinghofer, A. (2001).** Structural basis for guanine nucleotide exchange on Ran by the regulator of chromosome condensation (RCC1). *Cell* **105**, 245–55.

**Riddick, G. & Macara, I. G. (2005).** A systems analysis of importin-{alpha}-{beta} mediated nuclear protein import. *J Cell Biol* **168**, 1027–1038.

**Ritzi, M., Tillack, K., Gerhardt, J., Ott, E., Humme, S., Kremmer, E., Hammerschmidt, W. & Schepers, A. (2003).** Complex protein-DNA dynamics at the latent origin of DNA replication of Epstein-Barr virus. *J Cell Sci* **116**, 3971–3984.

**Schepers, A., Ritzi, M., Bousset, K., Kremmer, E., Yates, J. L., Harwood, J., Diffley, J. F. & Hammerschmidt, W. (2001).** Human origin recognition complex binds to the region of the latent origin of DNA replication of Epstein-Barr virus. *EMBO J* **20**, 4588–4602.

**Sears, J., Kolman, J., Wahl, G. M. & Aiyar, A. (2003).** Metaphase chromosome tethering is necessary for the DNA synthesis and maintenance of oriP plasmids but is insufficient for transcription activation by Epstein-Barr nuclear antigen 1. *J Virol* **77**, 11767–80.

**Sears, J., Ujihara, M., Wong, S., Ott, C., Middeldorp, J. & Aiyar, A. (2004).** The amino terminus of Epstein-Barr Virus (EBV) nuclear antigen 1 contains AT hooks that facilitate the

739 replication and partitioning of latent EBV genomes by tethering them to cellular
740 chromosomes. *J Virol* **78**, 11487–505.

741 **Shah, W. A., Ambinder, R. F., Hayward, G. S. & Hayward, S. D. (1992).** Binding of
742 EBNA-1 to DNA creates a protease-resistant domain that encompasses the DNA recognition
743 and dimerization functions. *J Virol* **66**, 3355–3362.

744 **Shire, K., Ceccarelli, D. F., Avolio-Hunter, T. M. & Frappier, L. (1999).** EBP2, a human
745 protein that interacts with sequences of the Epstein-Barr virus nuclear antigen 1 important for
746 plasmid maintenance. *J Virol* **73**, 2587–95.

747 **Tempera, I., De Leo, A., Kossenkov, A. V., Cesaroni, M., Song, H., Dawany, N., Showe,**
748 **L., Lu, F., Wikramasinghe, P. & Lieberman, P. M. (2015).** Identification of MEF2B,
749 EBF1, and IL6R as Direct Gene Targets of Epstein-Barr Virus (EBV) Nuclear Antigen 1
750 Critical for EBV-Infected B-Lymphocyte Survival. *J Virol* **90**, 345–355.

751 **Thomae, A. W., Pich, D., Brocher, J., Spindler, M.-P., Berens, C., Hock, R.,**
752 **Hammerschmidt, W. & Schepers, A. (2008).** Interaction between HMGA1a and the origin
753 recognition complex creates site-specific replication origins. *Proc Natl Acad Sci U S A* **105**,
754 1692-1697.

755 **Uchida, S., Sekiguchi, T., Nishitani, H., Miyauchi, K., Ohtsubo, M. & Nishimoto, T.**
756 **(1990).** Premature chromosome condensation is induced by a point mutation in the hamster
757 RCC1 gene. *Mol Cell Biol* **10**, 577–84.

758 **Wu, D. Y., Krumm, A. & Schubach, W. H. (2000).** Promoter-specific targeting of human
759 SWI-SNF complex by Epstein-Barr virus nuclear protein 2. *J Virol* **74**, 8893–8903.

760 **Wu, H., Kapoor, P. & Frappier, L. (2002).** Separation of the DNA replication, segregation,
761 and transcriptional activation functions of Epstein-Barr nuclear antigen 1. *J Virol* **76**, 2480–
762 2490.

763 **Wysokenski, D. A. & Yates, J. L. (1989).** Multiple EBNA1-binding sites are required to

764 form an EBNA1-dependent enhancer and to activate a minimal replicative origin within oriP
765 of Epstein-Barr virus. *J Virol* **63**, 2657–2666.
766 **Xiao, B., Verma, S. C., Cai, Q., Kaul, R., Lu, J., Saha, A. & Robertson, E. S. (2010).**
767 Bub1 and CENP-F can contribute to Kaposi's sarcoma-associated herpesvirus genome
768 persistence by targeting LANA to kinetochores. *J Virol* **84**, 9718–9732.
769 **Yates, J., Warren, N., Reisman, D. & Sugden, B. (1984).** A cis-acting element from the
770 Epstein-Barr viral genome that permits stable replication of recombinant plasmids in latently
771 infected cells. *Proc Natl Acad Sci U S A* **81**, 3806–3810.
772 **Yates, J. L. & Guan, N. (1991).** Epstein-Barr virus-derived plasmids replicate only once per
773 cell cycle and are not amplified after entry into cells. *J Virol* **65**, 483–488.
774 **Yates, J. L., Warren, N. & sugden, B. (1985).** Stable replication of plasmids derived from
775 Epstein-barr virus in various mammalian cells. *Nature* **313**, 812–815.
776 **Zhang, C., Goldberg, M. W., Moore, W. J., Allen, T. D. & Clarke, P. R. (2002).**
777 Concentration of Ran on chromatin induces decondensation, nuclear envelope formation and
778 nuclear pore complex assembly. *Eur J Cell Biol* **81**, 623–633.
779 **Zhang, M. S., Arnaoutov, A. & Dasso, M. (2014).** RanBP1 governs spindle assembly by
780 defining mitotic Ran-GTP production. *Dev Cell* **31**, 393–404.
781
782

## LEGENDS TO FIGURES

**Figure 1. Deletion of EBNA1 AT-hook domains drastically affects EBNA1-mediated transcriptional activation but has only moderate impact on EBV's association with the metaphasic chromosomes.** (A) Schematic representation of EBNA1 and AT-hook deletion mutants. Note: deletion coordinates shown are in the context of the GAr deletion (aa 93-325) and deletion of aa 1-7, incorporated in all constructs. GR: glycine/arginine-rich region; UR: unique region; GAr: glycine/alanine-repeat region; DBD: DNA-binding domain; NLS: nuclear localization signal; Ac: acidic. (B) Confocal microscopy analysis of EBNA1 and EBNA1 mutants during metaphase. HeLa cells were transfected with expression vectors for either GFP-EBNA1 or GFP-EBNA1 deletion mutants and the localization of the proteins was assessed in live cells by confocal microscopy. Upper and lower panels correspond to different individual cells. (C) FRAP analysis of EBNA1 and EBNA1 AT-Hooks deletion mutants expressed in HeLa cells. Average $t_{1/2}$ of fluorescence recovery was calculated from a minimum of 6 cells for each protein from a representative experiment. (D) HEK293T cells were transfected with the pGL2-FR-TK-Luc reporter plasmid, which contains the EBV FR-element cloned upstream of the Herpes simplex virus thymidine kinase (TK) promoter, either alone or together with expression vectors for EBNA1 or EBNA1 deletion mutants (as indicated). Luciferase activity was measured for identical amounts of total protein as evaluated by Bradford assay. Relative levels of luciferase activity are shown graphically. Error bars represent standard deviation from three replicate assays. Significant differences were evaluated by a student test (*** indicate a p value < 0,05; ns: non significant).

**Figure 2. EBNA1 and RCC1 interact directly. (**A) Expression plasmids for Flag-RCC1, Flag-EBNA1ΔGA, Myc-RCC1 and Myc-EBNA1ΔGA were transfected into HeLa cells as indicated. Cellular extracts were immunoprecipitated with anti-Flag affinity gel and the

immunoprecipitated complexes were analysed by western blotting using an anti-Flag polyclonal antibody or an anti-Myc antibody. Input corresponds to 8% of the cell extract used for immunoprecipitation. (B) 500 ng of purified 6xhis-EBNA1ΔGA protein were incubated with similar amounts of purified GST or GST-RCC1 bound to glutathione sepharose beads. The EBNA1-bound proteins were analysed by western blotting using an anti-his6 MAb. Input corresponds to 100 ng of purified 6xhis-EBNA1ΔGA.

**Figure 3. EBNA1 regions CBS-3, CBS-1 and CBS-2 are involved in the interaction with RCC1. (**A) Schematic representation of EBNA1. Abbreviations as in Figure 1 and CBS: chromosome binding sites. (B - C) Expression plasmids for GFP-tagged (B) or Flag-tagged (C) EBNA1 and EBNA1 deletion mutants, as indicated in the figure (note: protein/deletion coordinates shown are in the context of the GAr deletion (93-325) and deletion of aa 1-7, incorporated in all constructs), were transfected into HeLa cells. Cellular extracts were then incubated with similar amounts of GST or GST-RCC1 proteins bound to glutathione sepharose beads. Bound proteins were analysed by western blotting using either an anti-GFP antibody (B) or an anti-Flag antibody (C) as probes. Input corresponds to 10% of cell extract used for the GST-pulldown.

**Figure 4. Combined deletion of GR1 and GR2 drastically affects interaction with RCC1. (**A) Schematic representation of EBNA1 and EBNA1 deletion mutants. (B) Expression plasmids for GFP-tagged EBNA1 and EBNA1 deletion mutants, as indicated in the Figure, were transfected into HeLa cells. Cellular extracts were then incubated with similar amounts of GST or GST-RCC1 proteins bound to glutathione sepharose beads. Bound proteins were analysed by western blotting using an anti-GFP antibody as probe. Input corresponds to 10% of cell extract used for the GST-pulldown.

**Figure 5. RCC1 interacts with EBNA1 via its 20 amino acid N-terminal tail.**

(A) Schematic representation of RCC1. N- and C- terminal regions of RCC1 surround a seven bladed propeller domain (in grey). Residues 1 to 27 corresponding to the N-terminal tail are detailed below. The bi-partite NLS and phosphorylation sites on Ser 2 and 11 are indicated as well as the α-N-tri-methylation of serine 2 that follows cleavage of the first methionine indicated in brackets. (B) Expression plasmids for Flag-EBNA1 were transfected into HeLa cells and cellular extracts incubated with similar amounts of GST, GST-RCC1 or GST-RCC1-deletion mutants bound to glutathione sepharose beads, as indicated. Bound proteins were analysed by western blotting using an anti-Flag antibody. Input corresponds to 1/40 of the cell extract used for the GST-pulldown.

**Figure 6. Probing EBNA1 peptide arrays for RCC1 interaction sites.** (A) Arrays of immobilized peptide spots of overlapping 25-mer peptides covering the entire sequence of EBNA1 (including the GA repeat) were probed with recombinant GST-RCC1 (a), GST-RCC1Δ1-20 (b), GST-RCC1 1-20 (c) and GST (d) and revealed by incubation with an anti-GST antibody. Light blue, blue and red rectangles respectively indicate low, medium and high affinity binding to contiguous interacting peptides. The limits of the interacting regions are indicated for each rectangle by the positions of the first aa of the first peptide and the last aa of the last peptide. * Note: the GST-RCC1Δ1-20 array shown in the figure is the result of a longer exposure compared to the other array images. (B) Schematic representation of EBNA1 and its interaction regions with RCC1 as determined by the peptide array. Boxes along the linear depiction indicate binding (strong, intermediate or weak). Abbreviations are similar to those indicated in Figure 1. *indicates the position of the protein kinase 2 (CK2) binding sites. USP7: Ubiquitin Specific Peptidase 7. Positions of the AT-hook regions (between aa 40

to 53 and 326 to 358) are indicated in green.

**Figure 7. Dynamic localization of EBNA1 and RCC1 throughout the cell cycle.** HeLa cells coexpressing RFP-EBNA1 and EGFP-RCC1 were observed by confocal microscopy at different stages of the cell cycle as indicated. Images show single confocal z-section. Trans: Transmission.

**Figure 8. FRET analysis of EGFP-EBNA1 and RFP-RCC1 interaction at different stages of the cell cycle.** HeLa cells coexpressing EGFP-EBNA1 and RFP-RCC1 were analysed by Förster resonance energy transfer (FRET) at different stages of the cell cycle as indicated. Analyses were performed using ImageJ software 'FRET Analyzer'. Imaged cells were selected on the basis of both fusion proteins expression levels being similar to that found in single transfected cells used for spectral leakage calculation. Results are presented as three images, considering low, average or high spectral leakage level (noted as low, medium or high cut-off). High cut-off images are the most representative of the FRET signals. The FRET signal is represented using a firescale gradient: blue: no FRET signal, yellow: maximum FRET signal.

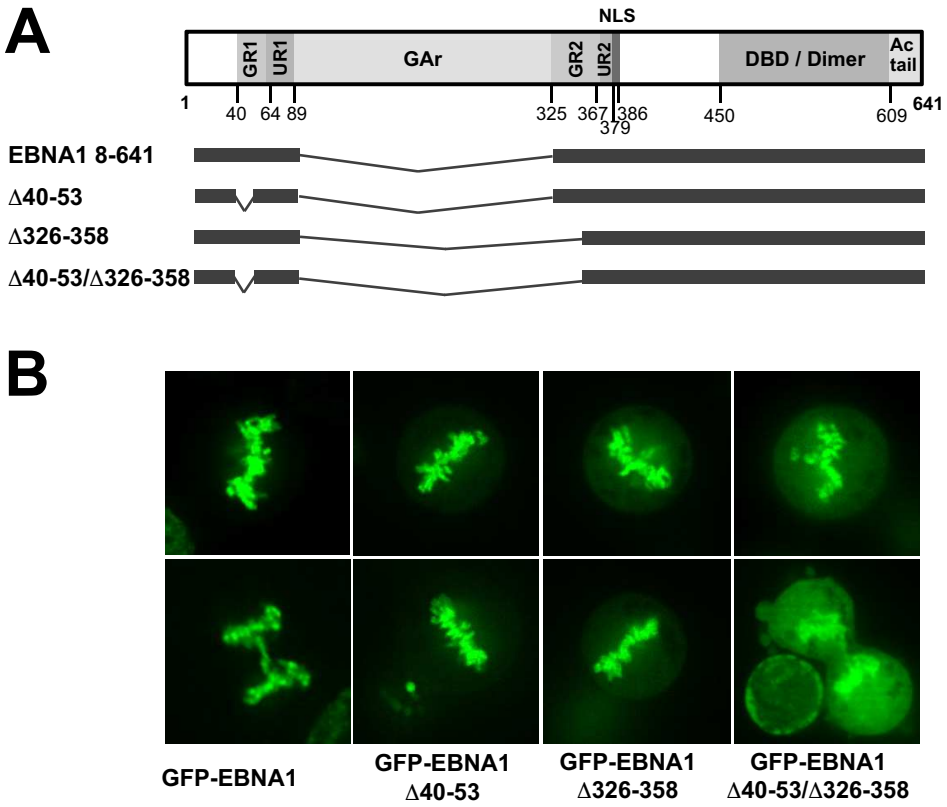

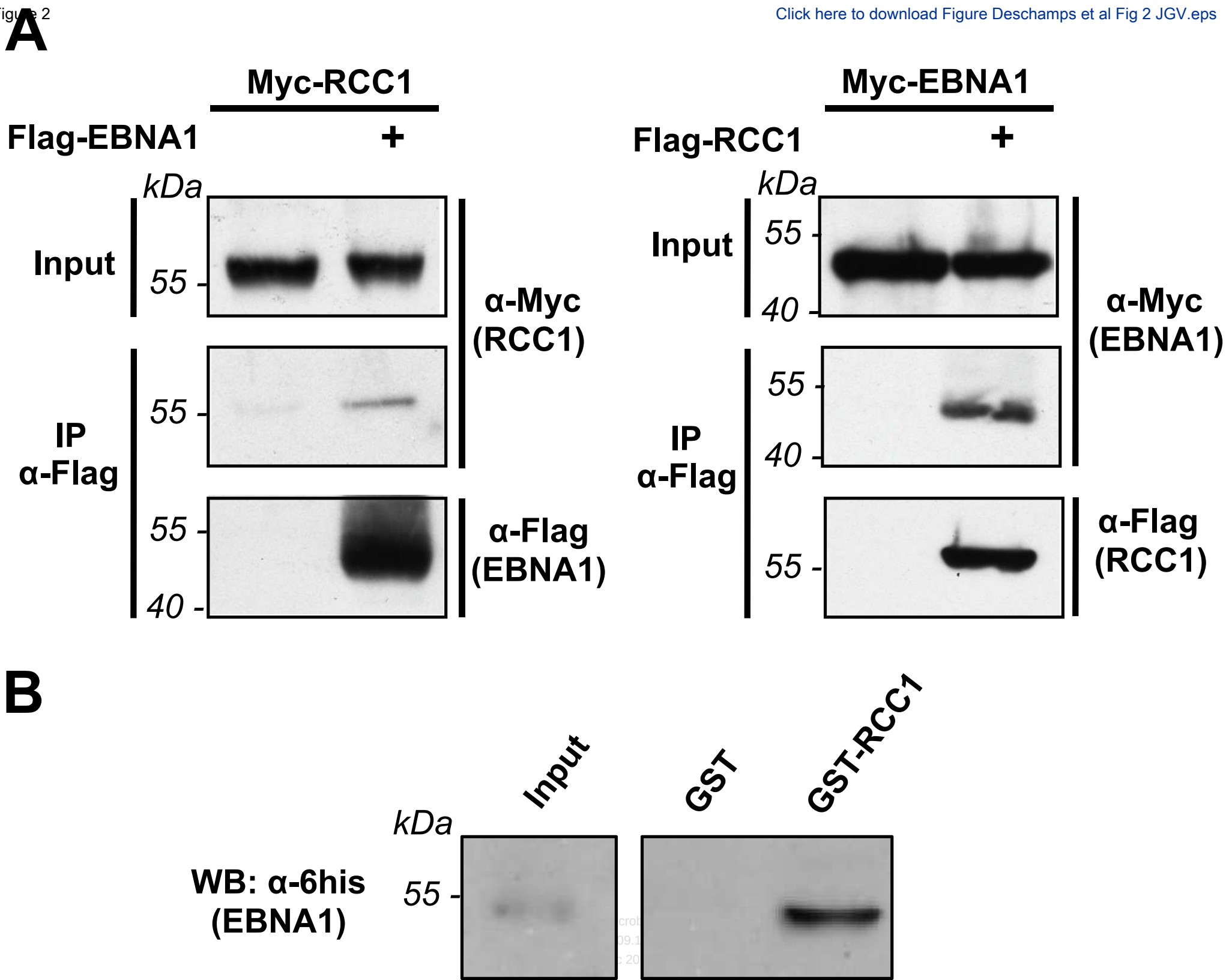

Figure 3



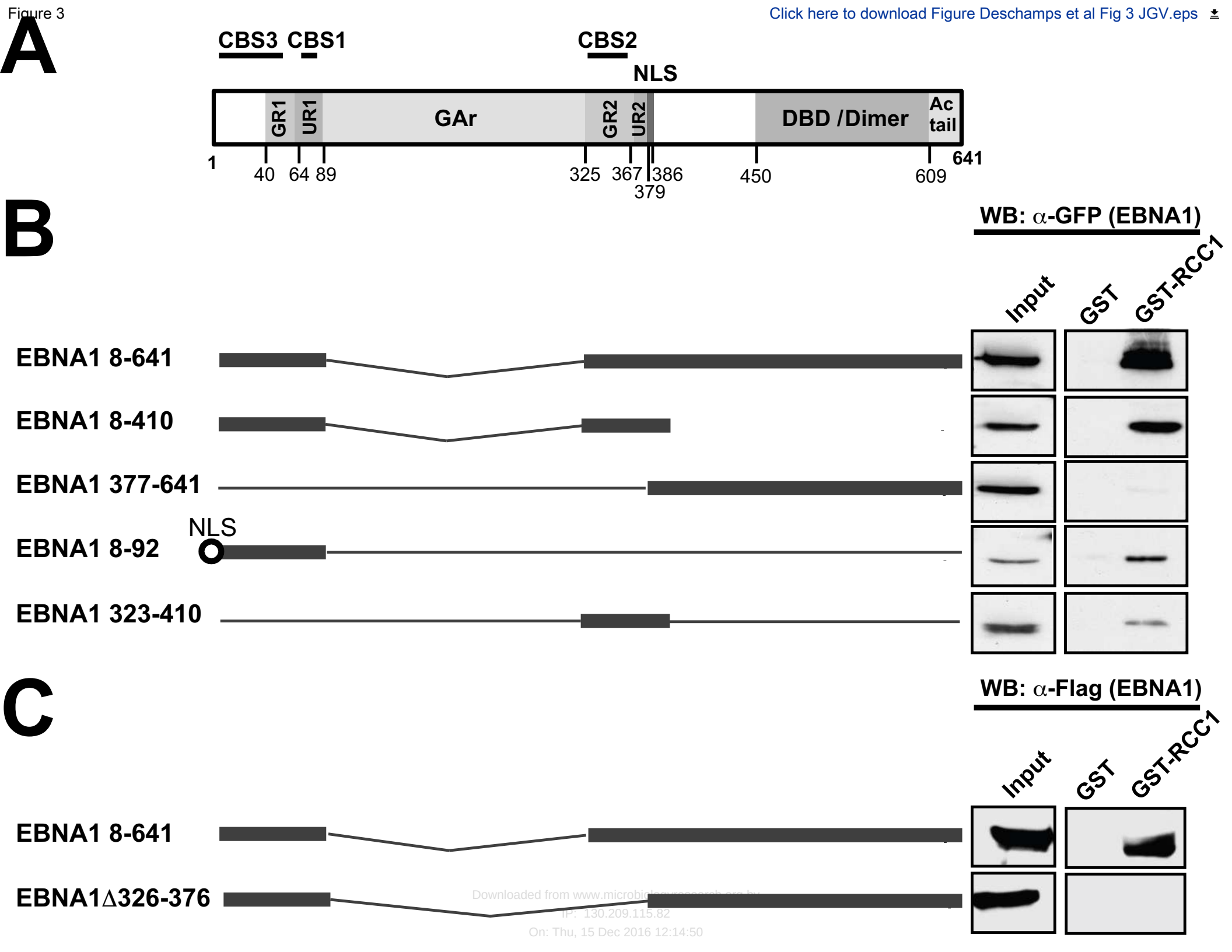

Figure 4



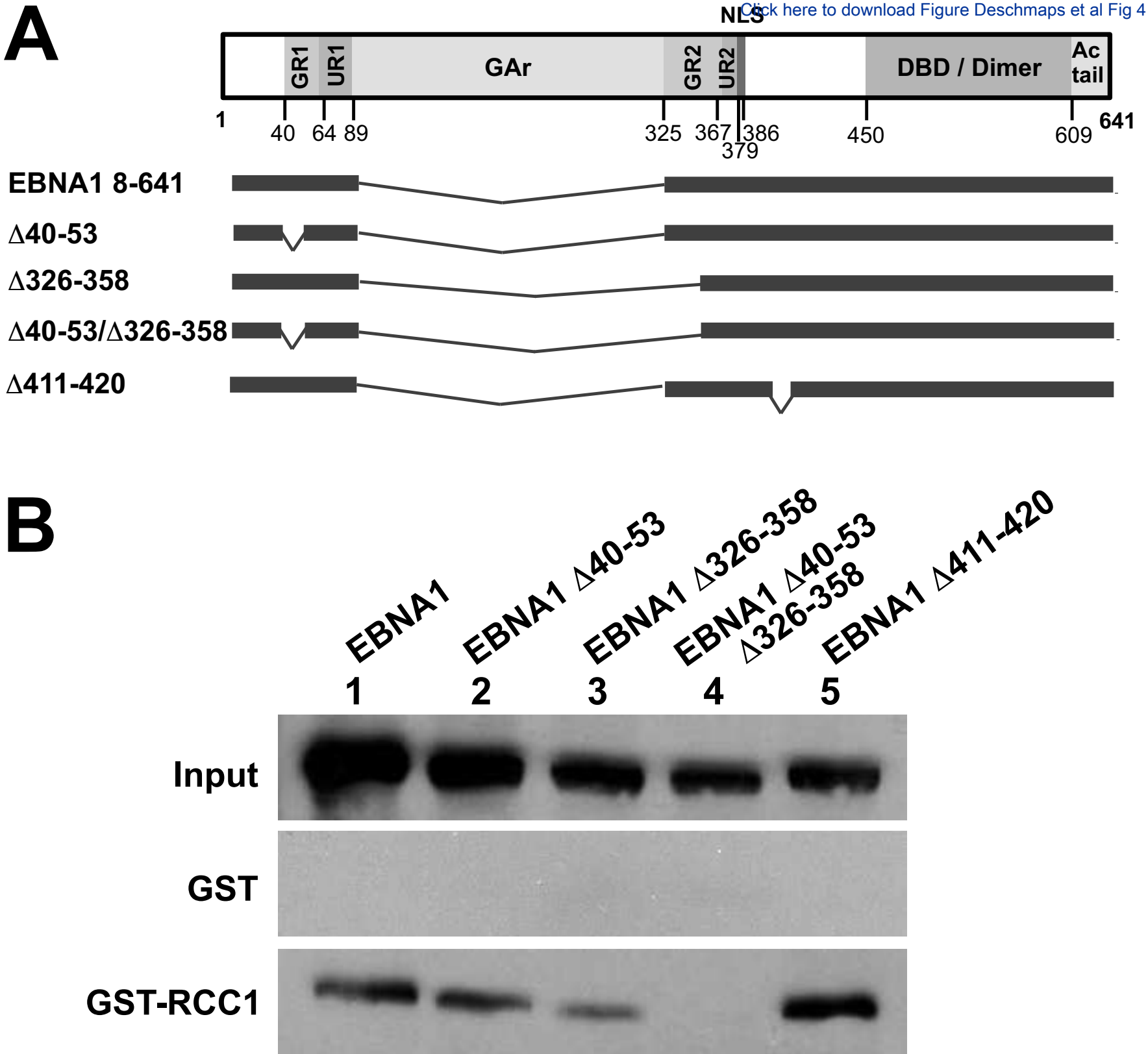

Figure 5



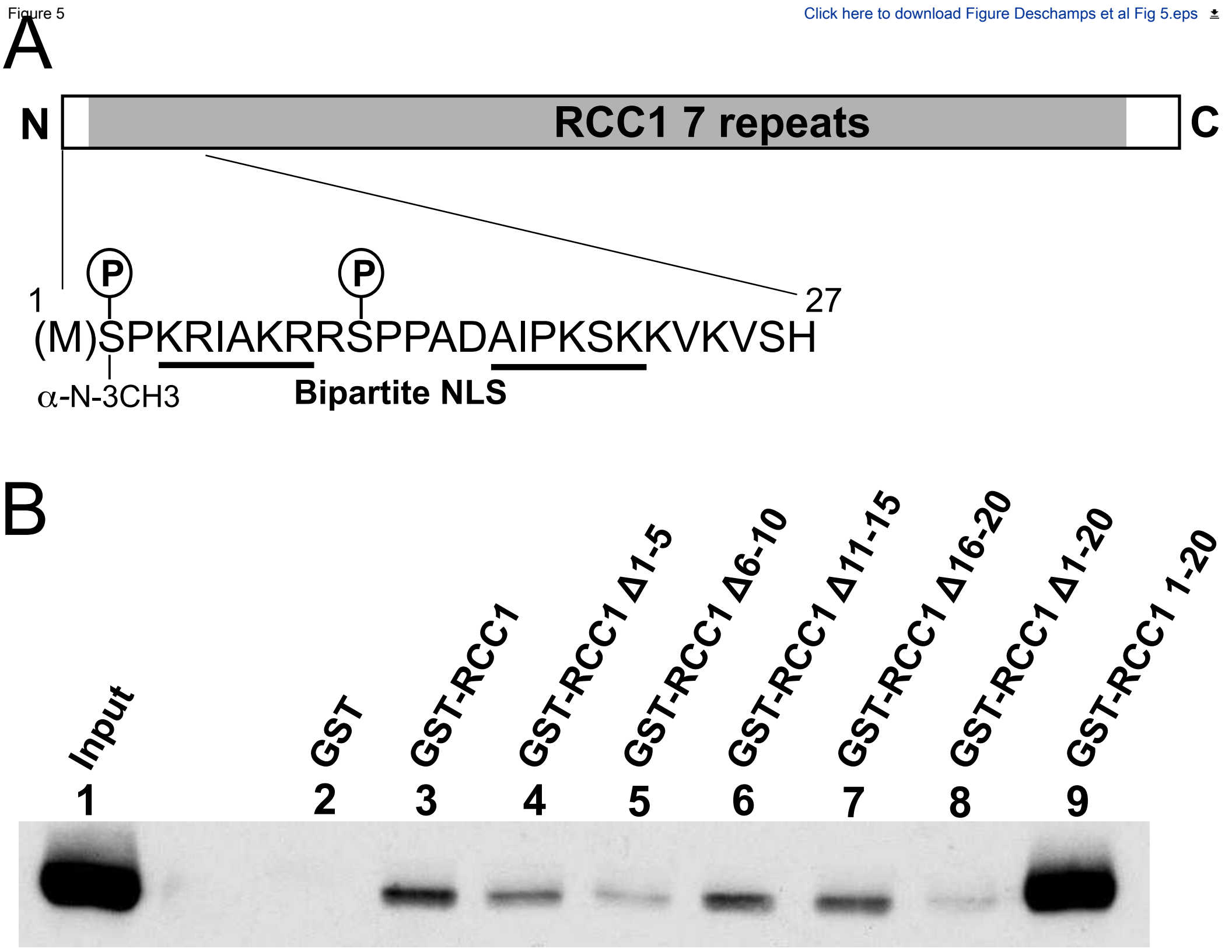

Figure 6



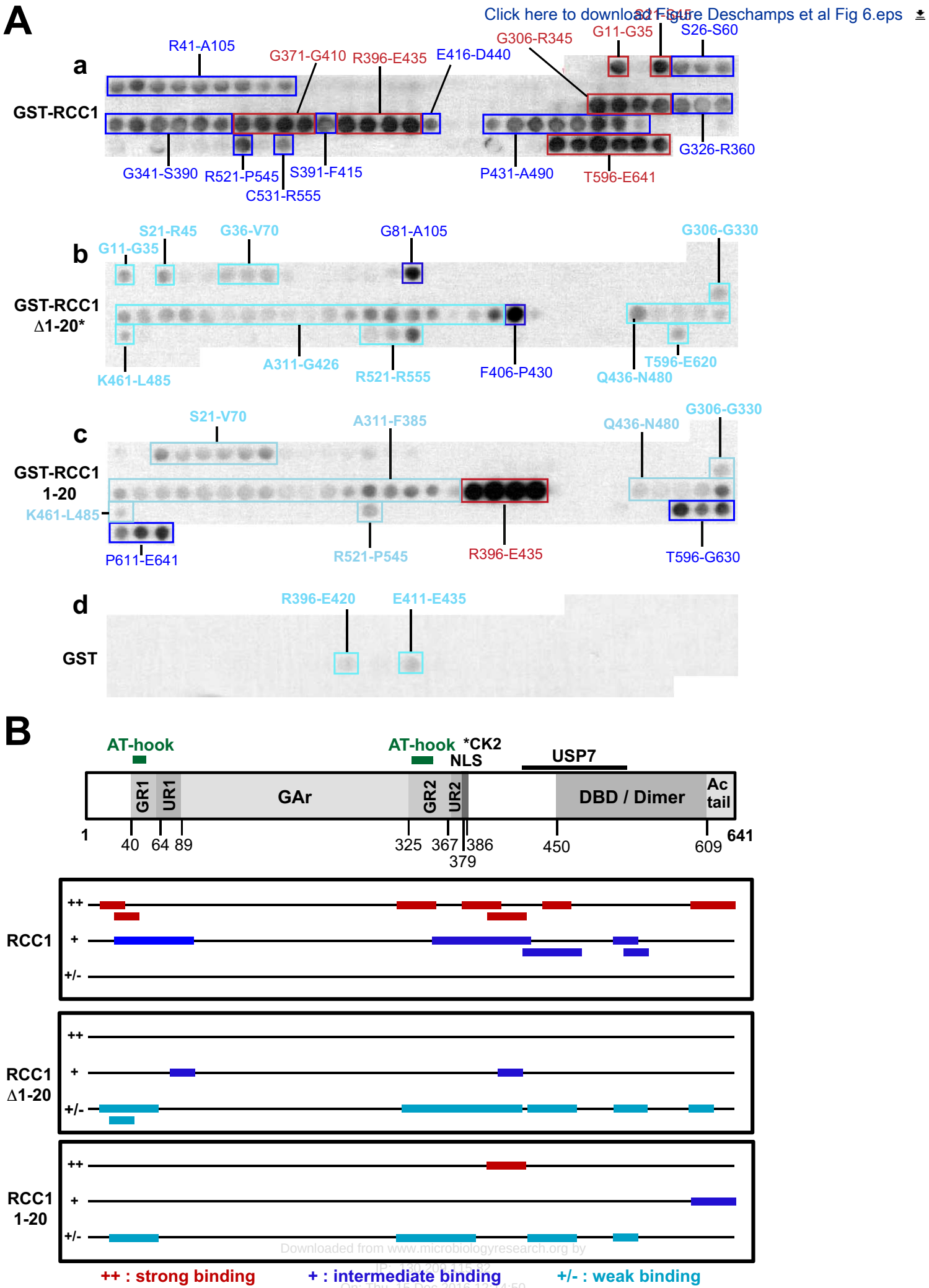

Figure 7



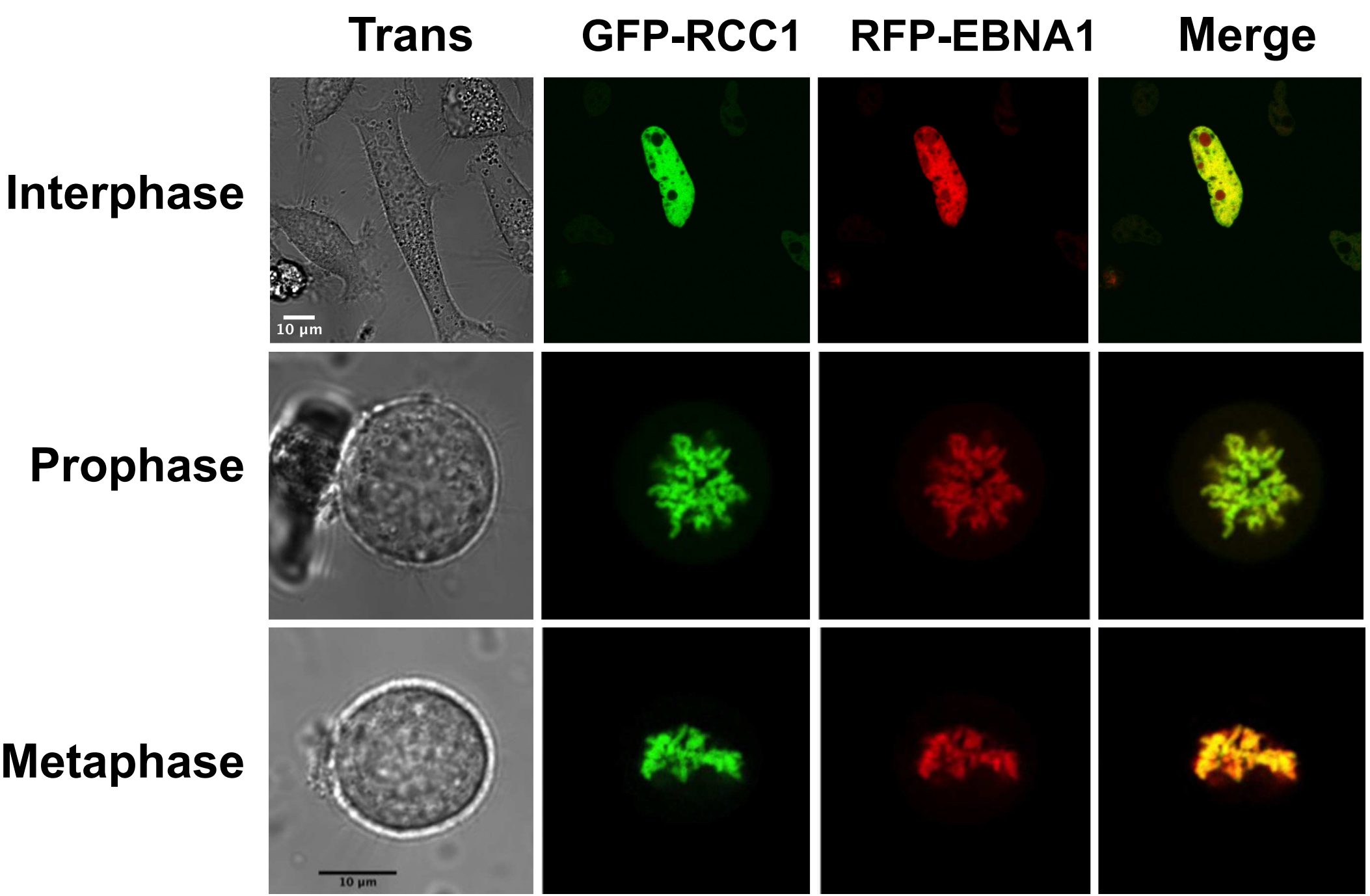

Figure 8



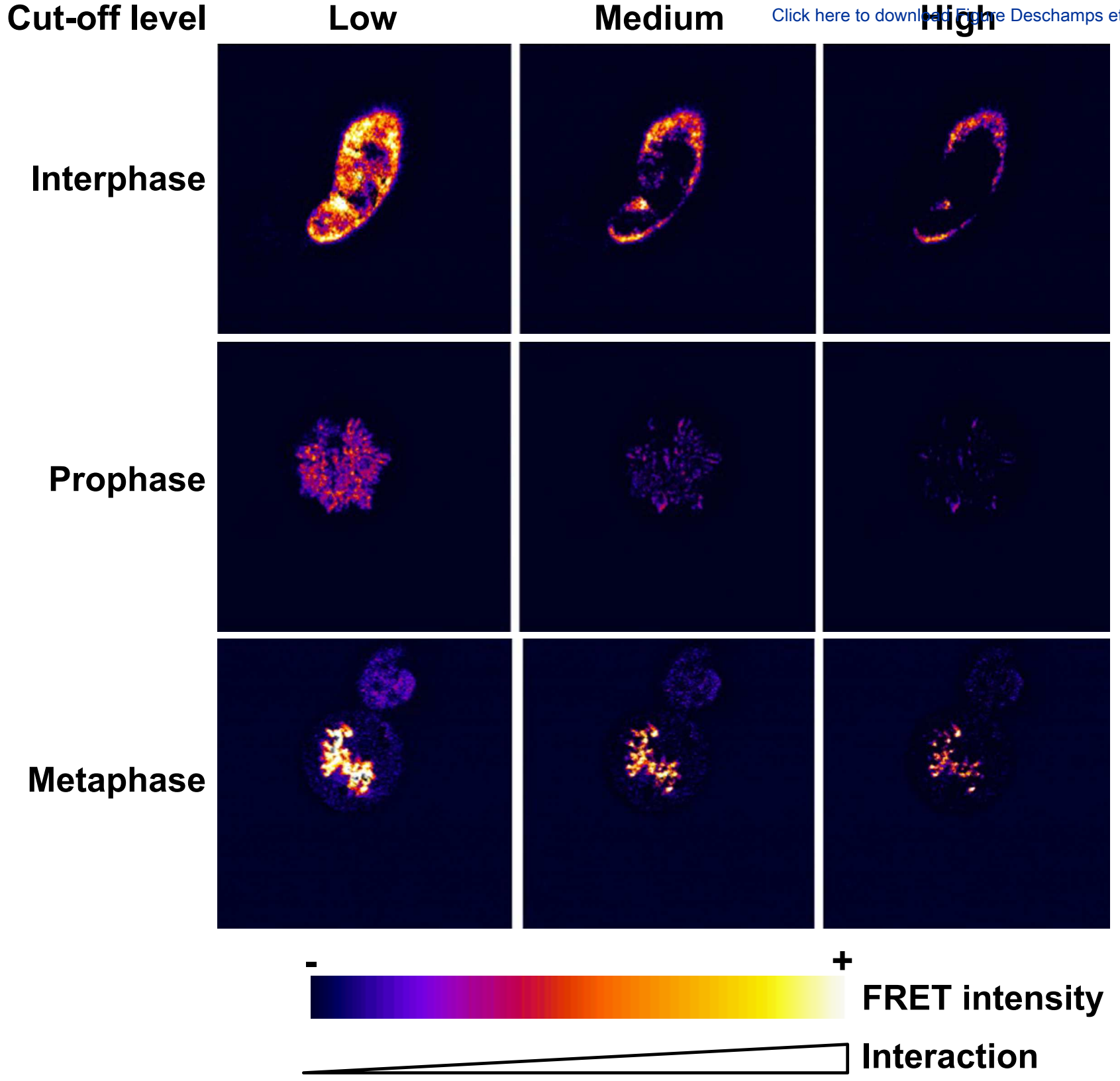

# SUPPLEMENTARY MATERIAL

## Legend to supplementary Figure 1.

The N-terminal region of RCC1 (MSPKRIAKRRSPPADAIPKS) contains 6 positively charged residues and one negatively charged residue. The C-terminal tail of EBNA1, from residue 610 to 641 has 14 negatively charged residues, interspersed with glycines and no positively charged residues. The stretch of residues in common between the EBNA1 peptides that span R396 to E435, which interact strongly with both RCC1 and RCC1 1-20, are aa 411 to 420 (EADYFEYHQE) and referred to below as the core region. This region contains 4 negatively-charged residues but is surrounded by residues of negative and positive charge.

To determine the key residues in this binding site, a new array was generated spanning the EBNA1 sequence from residue 401 to 430 and including a series of mutated peptides comprising: sequential Ala replacement peptides (Ala scanning); N- and C-terminal deletion peptides; Ala replacement of the four negatively-charged residues of the core region; and the core region alone (as shown). This array was probed with GST-RCC1 1-20. Sequential replacement of residues with Ala showed no (or little) reduction in binding until residue 413 (peptide 16). Ala replacement of DYFEY and Q of the core all showed substantial reduction in binding by GST-RCC1 1-20, with replacement of $F_{415}$ showing the weakest binding with these single replacements (peptides 16 to 20 and 22). Further Ala replacement to residue 430 (peptides 23 to 33) showed no reduction in binding, confirming the span of the core binding region. Replacement of the four charged residues ($E_{411}$, $D_{413}$, $E_{416}$, $E_{420}$) in the core completely abrogated binding (peptide 34), while binding to the 10 residue core alone (peptides 63 and 64) was as strong as binding to the full-length 25mer peptides incorporating this region. Sequential N-terminal deletion of the 25mer peptide revealed reduced binding upon deletion of $Y_{414}$ of the core and no binding with further N-terminal deletion, again revealing $F_{415}$ to be a critical residue in binding (peptides 43 to 48). It is noteworthy that this 15mer deleted up to $F_{415}$ still has 3 glutamate (negative) residues, but does not bind GST-RCC1 1-20. Sequential C-terminal deletion of the 25mer peptide (peptides 59 to 62) revealed reduced binding upon deletion of $E_{420}$, confirming the C-terminal limit of the core region. These data show that residues 413 to 420 (DYFEYHQE) of EBNA1 represent a tight binding region of the first 20 residues of RCC1, that the negatively charged residues in this region are essential for the interaction, and that $F_{415}$ and $Y_{414}$ are also key in the interaction.

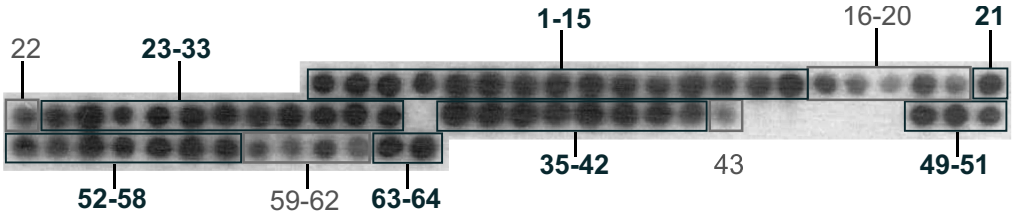


```
1  GRRPFFHPVGEADYFEYHQEGGPDG   ++
   ARRPFFHPVGEADYFEYHQEGGPDG   ++
   GARPFFHPVGEADYFEYHQEGGPDG   ++
   GRAPFFHPVGEADYFEYHQEGGPDG   ++
5  GRRAFFHPVGEADYFEYHQEGGPDG   ++
   GRRPAFHPVGEADYFEYHQEGGPDG   ++
   GRRPFAHPVGEADYFEYHQEGGPDG   ++
   FHPVGEADYFEYHQEGGPDGEPDVP   ++
   AHPVGEADYFEYHQEGGPDGEPDVP   ++
10 FAPVGEADYFEYHQEGGPDGEPDVP   ++
   FHAVGEADYFEYHQEGGPDGEPDVP   ++
   FHPAGEADYFEYHQEGGPDGEPDVP   ++
   FHPVAEADYFEYHQEGGPDGEPDVP   ++
   FHPVGAADYFEYHQEGGPDGEPDVP   ++
15 FHPVGEADYFEYHQEGGPDGEPDVP   ++
   FHPVGEAAYFEYHQEGGPDGEPDVP   +
   FHPVGEADAFEYHQEGGPDGEPDVP   +
   FHPVGEADYAEYHQEGGPDGEPDVP   +/-
   FHPVGEADYFAYHQEGGPDGEPDVP   +
20 FHPVGEADYFEAHQEGGPDGEPDVP   +
   FHPVGEADYFEYAQEGGPDGEPDVP   ++
   FHPVGEADYFEYHAEGGPDGEPDVP   +
   FHPVGEADYFEYHQAGGPDGEPDVP   ++
   FHPVGEADYFEYHQEAGPDGEPDVP   ++
25 FHPVGEADYFEYHQEGAPDGEPDVP   ++
   FHPVGEADYFEYHQEGGADGEPDVP   ++
   FHPVGEADYFEYHQEGGPAGEPDVP   ++
   FHPVGEADYFEYHQEGGPDAEPDVP   ++
   FHPVGEADYFEYHQEGGPDGAPDVP   ++
30 FHPVGEADYFEYHQEGGPDGEADVP   ++
   FHPVGEADYFEYHQEGGPDGEPAVP   ++
   FHPVGEADYFEYHQEGGPDGEPDAP   ++
   FHPVGEADYFEYHQEGGPDGEPDVA   ++
   FHPVGAAAYFAYHQAGGPDGEPDVP   -

35 HPVGEADYFEYHQEGGPDGEPDVP   ++
     PVGEADYFEYHQEGGPDGEPDVP   ++
      VGEADYFEYHQEGGPDGEPDVP   ++
       GEADYFEYHQEGGPDGEPDVP   ++
        EADYFEYHQEGGPDGEPDVP   ++
40       ADYFEYHQEGGPDGEPDVP   ++
          DYFEYHQEGGPDGEPDVP   ++
           YFEYHQEGGPDGEPDVP   ++
            FEYHQEGGPDGEPDVP   +/-
             EYHQEGGPDGEPDVP   -
45            YHQEGGPDGEPDVP   -
               HQEGGPDGEPDVP   -
                QEGGPDGEPDVP   -
                 EGGPDGEPDVP   -
   FHPVGEADYFEYHQEGGPDGEPDV    ++
50 FHPVGEADYFEYHQEGGPDGEPD     ++
   FHPVGEADYFEYHQEGGPDGEP      ++
   FHPVGEADYFEYHQEGGPDGE       ++
   FHPVGEADYFEYHQEGGPDG        ++
   FHPVGEADYFEYHQEGGPD         ++
55 FHPVGEADYFEYHQEGGP          ++
   FHPVGEADYFEYHQEGG           ++
   FHPVGEADYFEYHQEG            ++
   FHPVGEADYFEYHQE             ++
   FHPVGEADYFEYHQ              +/-
60 FHPVGEADYFEYH               +/-
   FHPVGEADYFEY                +
   FHPVGEADYFE                 +/-
        EADYFEYHQE             ++
   FHPVGEADYFEYHQEGGPDGEPDVP   ++
```

**Supplementary Figure 1. Characterization of amino acids within EBNA1 region 401 to 430 that show strong interaction with the RCC1 N-terminal 20 amino acid tail.**

| Construction name | Primers for gateway cloning |
|---|---|
| pDONR-EBNA1 | 5’-GGGGACAACTTTGTACAAAAAAGTTGGCATGACAGGACCTGCAAATGGCC-3’<br>5’-GGGGACAACTTTGTACAAGAAAGTTGGTCACTCCTGCCCTTCCTCAC-3’ |
| pDONR-EBNA1 8-410 | 5’-GGGGACAACTTTGTACAAAAAAGTTGGCATGACAGGACCTGCAAATGGCC-3’<br>5’-GGGGACAACTTTGTACAAGAAAGTTGGTCACCCTACAGGGTGGAAAAATGG-3’ |
| pDONR-EBNA1 381-Cter | 5’-GGGGACAACTTTGTACAAAAAAGTTGGCATGCCCAGGAGTCCCAGTAGTCAG-3’<br>5’-GGGGACAACTTTGTACAAGAAAGTTGGTCACTCCTGCCCTTCCTCAC-3’ |
| pDONR-RCC 1-20 | 5’-GGGGACAACTTTGTACAAAAAAGTTGGCATGTCACCCAAGCG-3’<br>5’-GGGGACAACTTTGTACAAGAAAGTTGGTTAGCTTTTGGGGATGGC-3’ |
| pDONR-EBNA1 8-92nls | 5’-GGGGACAACTTTGTACAAAAAAGTTGGCATGCCTAAGAAGAAGCGCAAAGTC<br>GGACCTGGAAATGGCC-3’<br>3’-GGGGACAACTTTGTACAAGAAAGTTGGTCATCCTGCTCCTGTTCCACCG-5’ |
| pDONR-EBNA1 323-410 | 5’-GGGGACAACTTTGTACAAAAAAGTTGGCATGGAGCAGGAGGTGGAGGC-3’<br>5’-GGGGACAACTTTGTACAAGAAAGTTGGTCACCCTACAGGGTGGAAAAATGG-3’ |
| | Primers for Infusion cloning |
| pRFP-N1-EBNA1 | 5’-GGCAGGAGAAGGATCCGGCCTCCTCCGAGGACGTCATC-3’<br>5’-TCTAGAGTCGCGGCCGCGCAGAATTCTTAGGCGCCGGTGGA-3’ |
| pRFP-C1-EBNA1 | 5’-CGCTAGCGCTACCGGTGAGCTCGGATCCATGGCCTCC 3’<br>5’-TCCAGGTCCTGTATCTGCAGTTCTATAGGCGCCGGTGGAGTG 3’ |
| peGFP-N1-RCC1 | 5’-CTCAAGCTTCGAATTC ATGTCACCCAAGCGCATAG-3’<br>5’-GGCGACCGGTGGATCC GCTCTGTTCTTTGTCCTTGACTAA-3’ |
| peGFP-C1-RCC1 | 5’-TCAAGCTTCGAATTCTGCAGGGACTTTCCCCAGCACAGCCAGCATGT-3’<br>5’-GCACGCATGATGTCTACTCACTCGGCAGGCGGGGGACATTC -3’ |
| pRFP-N1-RCC1 | 5’-GGACTCAGATCTCGAGATGTCACCCAAGCGCATAGC-3’<br>5’-GGAGGAGGCCGGATCC**CC**GCTCTGTTCTTTGTCCTTGAC-3’ |
| pRFP-C1-RCC1 | 5’-CGCTAGCGCTACCGGTATGGCCTCCTCCGAGGACG-3’<br>5’-GAAGCTTGAGCTCGAGCGCCGGTGGAGTGGCG |
| | Primers for site directed mutagenesis |
| peGFP-N1-EBNA1 Δ40-53 | 5'-GGGGCTCCTGGATGGTTATCACCCCCTCTT-3' |

| | |
|---|---|
| | 5'-AAGAGGGGGTGATAACCATCCAGGAGCCCC-3' |
| peGFP-N1-EBNA1 Δ326-358 | 5'-CACGGTGGAACAGGAGAAAGAGCCAGGGGG-3'<br>5'-CCCCCTGGCTCTTTCTCCTGTTCCACCGTG-3' |
| peGFP-N1-EBNA1 Δ411-420 | 5'-CCACCCTGTAGGGGGTGGCCCAGATGGTG-3'<br>5'-CACCATCTGGGCCACCCCCTACAGGGTGG-3' |
| pDEST15-RCC1 Δ1-20 | 5'-GTACAAAAAAGTTGGCATAGCTAAAAGAAGGTCCC-3'<br>5'- GAGACCTTCACCTTCTTATCTGCTGGGG-3' |
| pDEST15-RCC1 Δ1-5 | 5'-GTACAAAAAAGTTGGCATAGCTAAAAGAAGGTCCC-3'<br>5'-GGGACCTTCTTTTAGCTATGCCAACTTTTTTGTAC-3' |
| pDEST15-RCC1 Δ6-10 | 5'-GCATGTCACCCAAGCGCTCCCCCCCAGCAGATGC-3'<br>5' GCATCTGCTGGGGGGGAGCGCTTGGGTGACATGC-3' |
| pDEST15-RCC1 Δ11-15 | 5'-GCATAGCTAAAAGAAGGGCCATCCCCAAAAGC-3'<br>5'- GCTTTTGGGGATGGCCCTTCTTTTAGCTATGC-3' |
| pDEST15-RCC1 Δ16-20 | 5'-CCCCAGCAGATAAGAAGGTGAAGGTCTC-3'<br>5'- GAGACCTTCACCTTCTTATCTGCTGGGG-3' |

**Supplementary table :** Oligonucleotides used for PCR-amplifications, Infusion cloning and Site-Directed mutagenesis.